



**ECONOMIC GEOLOGY
RESEARCH UNIT**

University of the Witwatersrand
Johannesburg

THE SERPENTINITES AND RELATED ROCKS OF THE
MSAULI ASBESTOS DEPOSIT IN THE ARCHAEOAN
BARBERTON GREENSTONE BELT, SOUTH AFRICA

W. BÜTTNER

INFORMATION CIRCULAR NO. 168

UNIVERSITY OF THE WITWATERSRAND
JOHANNESBURG

THE SERPENTINITES AND RELATED ROCKS OF THE MSAULI ASBESTOS
DEPOSIT IN THE ARCHAEOAN BARBERTON GREENSTONE BELT, SOUTH AFRICA

by

W. BÜTTNER

*(Mineralogisch-Petrographisches Institut
Universität zu Köln, West Germany)*

ECONOMIC GEOLOGY RESEARCH UNIT
INFORMATION CIRCULAR NO. 168

February, 1984

THE SERPENTINITES AND RELATED ROCKS OF THE MSAULI ASBESTOS
DEPOSIT IN THE ARCHAEN BARBERTON GREENSTONE BELT, SOUTH AFRICA

ABSTRACT

The Msauli ultramafic body, consisting of serpentinites and their alteration products, together with metapyroxenites, metagabbros, and rodingites, is situated in the uppermost formation of the volcanic Onverwacht Group in the south-eastern part of the Archaean Barberton greenstone belt. The serpentinites are largely formed by olivine pseudomorphs, which consist of lizardite, mainly as a α -serpentine in the footwall serpentinite (FWS) and hanging wall serpentinite (HWS), and as γ -serpentine in the ore zone serpentinite (OZS). Cross-fibre chrysotile, which forms economic asbestos grades, is concentrated towards the OZS. In addition to large quantities of chrysotile, the OZS also contains appreciable amounts of brucite. Near the 'stratigraphic' base of the Msauli ultramafic intrusion the serpentine minerals are largely replaced by magnesite, talc, quartz, and chlorite, thus forming the footwall alteration zone. The serpentinites are 'stratigraphically' overlain by metapyroxenites, metagabbros and rodingites. Near their margins the metagabbros possess spinifex textures, suggesting rapid cooling of the magma. The emplacement of the Msauli ultramafic body took place either as a shallow sill-like intrusion under sub-sea-floor conditions, or as a submarine ultramafic lava flow. Circulating sea water caused the hydrothermal alteration of the pyroxenitic and gabbroic rocks, as well as a first stage of serpentinization in the dunitic zone (FWS and HWS) of the Msauli ultramafics. The second stage of serpentinization affected the central part of the dunitic zone (OZS) and occurred under a low temperature regime, after the folding of the Barberton greenstone belt. Probably still during the second serpentinization stage, the Northern Porphyry, a felsic porphyry intrusion, was emplaced in the vicinity of the Msauli ultramafic body and thereby caused the fracture system in the OZS in which the asbestos-forming cross-fibre chrysotile crystallized. Mineralizing solutions stemmed from the continuing process of serpentinization of olivine in the OZS and from pressure solution effects. The formation of the footwall alteration zone took place after the formation of the cross-fibre as a result of the introduction of CO_2 -rich hydrothermal solutions. Although differences exist between ophiolites and the Msauli ultramafic body, the latter can be regarded as an Archaean equivalent of a Phanerozoic ophiolite.

* * *

THE SERPENTINITES AND RELATED ROCKS OF THE MSAULI ASBESTOS
DEPOSIT IN THE ARCHAEN BARBERTON GREENSTONE BELT, SOUTH AFRICA

CONTENTS

	<u>Page</u>
I. <u>INTRODUCTION</u>	1
II <u>GEOLOGIC SETTING</u>	1
III. <u>MSAULI ULTRAMAFIC BODY</u>	4
A. Serpentinites	6
1. <i>Lithology</i>	6
2. <i>Mineralogy</i>	7
B. Footwall Alteration Zone	12
C. Hanging Wall Zone	13
D. Chemistry	16
1. <i>Serpentine Chemistry</i>	16
2. <i>Whole Rock Geochemistry</i>	21
IV. <u>DISCUSSION</u>	21
V. <u>CONCLUSIONS</u>	27
<u>ACKNOWLEDGMENTS</u>	28
<u>REFERENCES</u>	28

— 000 —

Published by the Economic Geology Research Unit
University of the Witwatersrand
1 Jan Smuts Avenue
Johannesburg 2001

ISBN 0 85494 816 3

THE SERPENTINITES AND RELATED ROCKS OF THE MSAULI ASBESTOS
DEPOSIT IN THE ARCHAEN BARBERTON GREENSTONE BELT, SOUTH AFRICA

I. INTRODUCTION

Most asbestos-bearing serpentinites throughout the world are confined to Phanerozoic mountain belts. This is particularly the case for the major asbestos deposits in Canada, USSR, Australia, and Italy. By contrast the Msauli asbestos deposit, sited in the Barberton greenstone belt of South Africa (Fig. 1), provides an opportunity to study a chrysotile deposit which lies in Archaean low grade metamorphic rocks.

Although South Africa is a major asbestos producer, ranking third in the world, most of the asbestos mined consists of crocidolite (Cape blue). The Msauli asbestos mine, therefore, is one of the few producers of chrysotile asbestos in South Africa, with an annual fibre production of some 90000 tons (Büttner and Saager, 1982a).

Mining of the Msauli deposit began in 1942 when some asbestos ore outcrops were discovered near the Msauli River. In subsequent years the mining operations were continuously extended and the mining method changed from open pit to underground mining. A geological study of the Msauli deposit and its surroundings was conducted between 1979 and 1980 and was followed by detailed petrological and geochemical investigations (Büttner, 1983a).

Another chrysotile asbestos deposit, in a geological setting similar to that of the Msauli deposit, occurs at the Havelock Mine in Swaziland, just 7 km north-east of the Msauli ore body. Still other deposits of this type occur on the north-western flank of the Barberton greenstone belt (van Biljon, 1964; Anhaeusser, 1976) and in some greenstone belts in Zimbabwe (Laubscher, 1964).

II. GEOLOGIC SETTING

The Barberton greenstone belt consists of three major stratigraphic units. At the base are volcanic rocks of the Onverwacht Group, followed by argillaceous sediments of the Fig Tree Group and arenaceous sediments of the Moodies Group at the top of the succession. These three units together form the Barberton Sequence of the Swaziland Supergroup. Radiometric age determinations have established the time interval for the deposition of the Barberton Sequence to be between 3,5 and 3,3 Ga ago (Barton, 1983; Hamilton *et al.*, 1979; Jahn *et al.*, 1982). Additional details concerning the geology and evolution of the Barberton greenstone belt are provided by Anhaeusser (1978, 1981a,b) and Viljoen and Viljoen (1969a-c).

The Msauli ultramafic intrusion which contains the Msauli asbestos deposit, is situated in a structurally complex area in the south-eastern part of the Barberton greenstone belt (Fig. 2). This area comprises the two uppermost formations of the Onverwacht Group, namely the Kromberg and Swartkoppie formations, together with the Fig Tree Group and parts of the Moodies Group. Viljoen and Viljoen (1969c) suggested that in this area the Kromberg and Swartkoppie formations are divided by a major fault zone, the

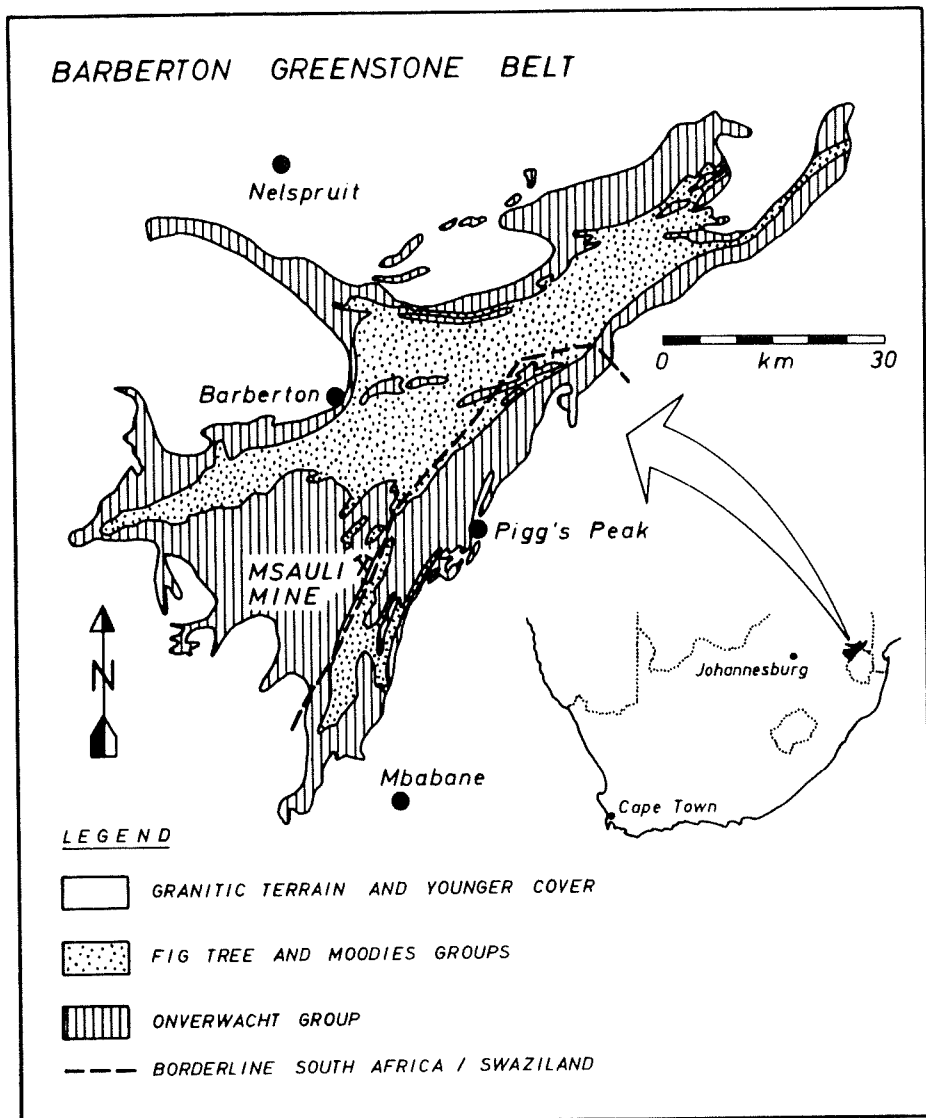


Figure 1 : Generalized geological map of the Barberton greenstone belt in South Africa, and the locality of the Msauli asbestos mine.

Maanhaar Fault. Their findings were confirmed by Büttner (1983a) who showed that the directions of younging of the successions are different on both sides of the Maanhaar Fault, and that the Kromberg Formation is folded into an isoclinal syncline with a fold axis dipping gently towards north-north-east.

Lithologically, the Kromberg and Swartkoppie formations consist of basic to felsic metavolcanics. Basic metalavas, often with conspicuous pillow structures, predominate in the Kromberg Formation which also reflects a magmatic cyclicity. Each cycle commences with basic lavas at the base, gradually becoming felsic towards the top of the cycle. The individual cycles are usually terminated by a chert horizon, which, according to Lowe and Knauth (1977), consists of silicified volcanogenic debris.

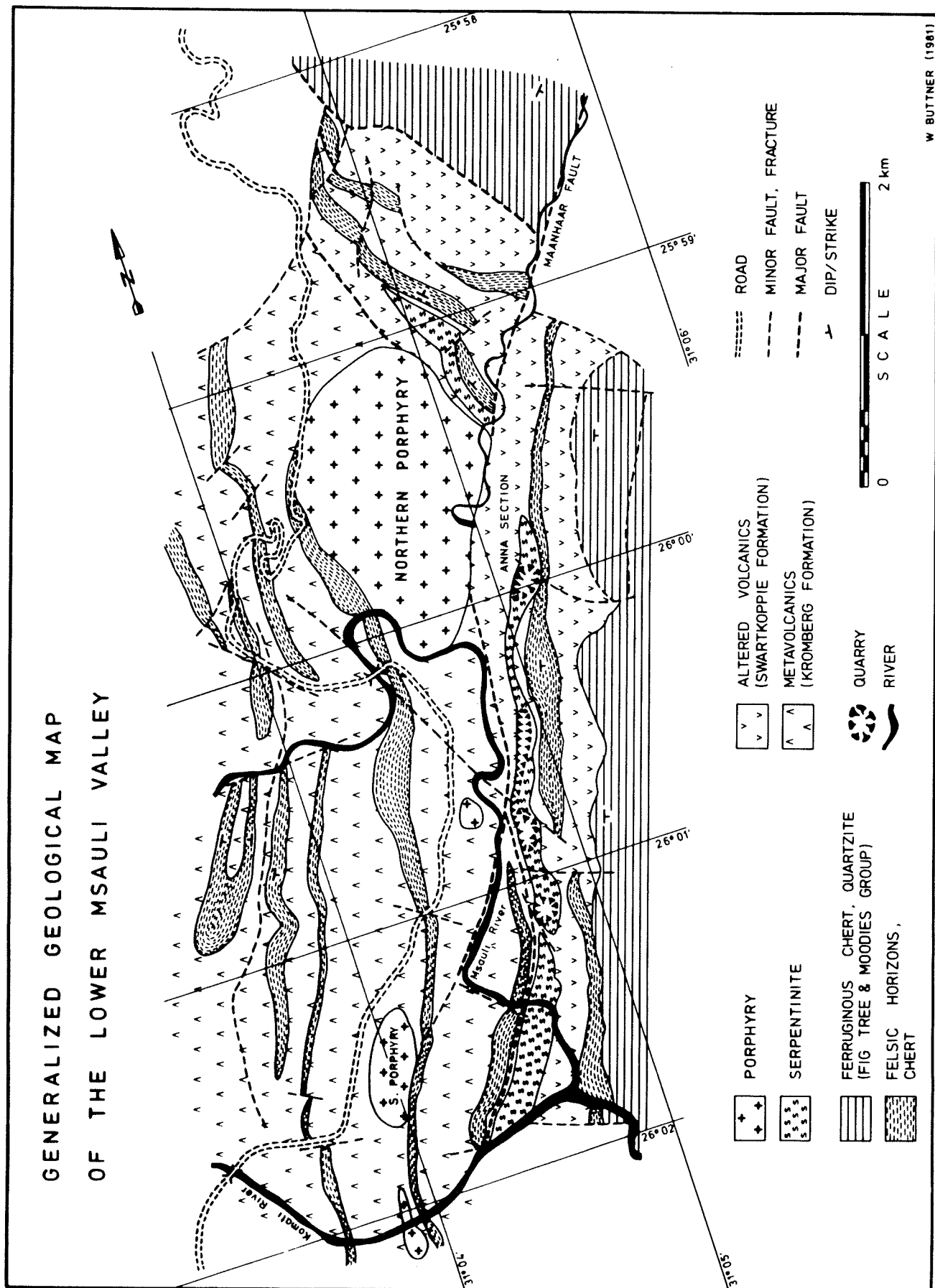


Figure 2 : Geological map of the Lower Msauli valley showing the distribution of the Msauli ultramafic body (marked as serpentinite).

As mentioned above, the Swartkoppie Formation lies in tectonic contact with the Kromberg Formation (Fig. 2). The actual stratigraphic relationship between these two formations is not clear. Heinrichs (1980), following regional mapping carried out in the area, suggested that the Swartkoppie Formation may in fact be the uppermost part of the Kromberg Formation which has been tectonically separated from the lower beds.

Because of poor outcrops it is difficult to characterize the Swartkoppie Formation in the vicinity of the Msauli Mine. Underground exposures and some surface outcrops indicate that the Swartkoppie Formation consists mainly of intermediate-to-felsic metavolcanics, including altered tuffs. Mineralogical investigations showed that these rocks consist mainly of quartz, dolomite, sericite, albite, tremolite, and chlorite. The upper sequence of the Swartkoppie Formation is terminated by the Swartkoppie chert (Heinrichs, 1980; Eriksson, 1980), a prominent chert horizon which locally attains a thickness of approximately 200 m. Structural features, such as drag folds, suggest that the Swartkoppie Formation has been partly subjected to thrusting and sub-parallel gliding along bedding planes.

Conformably overlying the Swartkoppie Formation are banded iron-formation of the Fig Tree Group which consist of thinly-bedded, alternating quartz- and iron-rich layers. Principal iron-bearing minerals in these rocks are hematite and magnetite. Interlayered with and overlying the banded iron-formation are shales, cherts, greywackes, grits and sandstones. The sandstones and grits grade progressively into the basal conglomerate of the Moodies Group which terminates the stratigraphic succession in the area investigated (Fig. 2).

Ultramafic complexes similar to the Msauli ultramafic body, are common throughout the Barberton greenstone belt (Anhaeusser, 1976, 1983; Viljoen and Viljoen, 1969c, 1970). Many of them are thought to occur as conformable sill-like intrusives but others have an irregular shape and display discordant relationships with the surrounding country rocks. Such an unconformable ultramafic body of wehrlitic composition was found some 5 km south-west of the area depicted in Fig. 2.

A number of intrusive felsic porphyries occur close to the Maanhaar fault zone. Their age, geochemistry and origin has been investigated by Büttner *et al.*, (1983). The largest of these porphyry stocks, known as the Northern Porphyry, is situated close to the Msauli mining area. Rb-Sr whole rock isotopic analyses yielded an emplacement age for the porphyry of 2766 Ma with an initial $^{87}\text{Sr}/^{86}\text{Sr}$ ratio of 0.7059 (Büttner *et al.*, 1983).

Latest magmatic events recorded in the vicinity of the Msauli ultramafic body comprise at least two generations of intermediate-to-mafic dykes but the latter have not been included on the map (Fig. 2) for the sake of clarity.

III. MSAULI ULTRAMAFIC BODY

The Msauli ultramafic body occurs as an approximately conformable lens, interlayered in beds of the Swartkoppie Formation that dip steeply ($\pm 70^\circ$) to the east-south-east. In Fig. 2 the Msauli intrusion is shown as a serpentinite body outcropping over a strike length of approximately 4 km. Drilling results have confirmed that the serpentinites do not continue south of the Komati River where the area is thickly covered by alluvial sediments.

The southern extension of the Msauli ultramafic body, if it existed, was probably sheared off along transverse faults during the folding of the Barberton greenstone belt, and may later have been removed by erosion. The Msauli serpentinite has a thickness of approximately 200 m and, in the mining areas, has been traced down to a depth of about 400 m. Tectonic activity related to the folding of the Barberton greenstone belt has caused local thinning of the serpentinites along strike.

Three lithologically different zones can be distinguished in the Msauli ultramafic body. These include: (i) the footwall alteration zone; (ii) the serpentinite zone, and (iii) the hanging wall zone. The *footwall alteration zone* consists of chlorite-talc-carbonate rocks, quartz-carbonate rocks, and talc-carbonate rocks, which often possess schistose textures. The serpentinites of the *serpentinite zone* have been further subdivided mineralogically, as well as according to their spatial distribution, into footwall serpentinite (FWS), ore zone serpentinite (OZS), and hanging wall serpentinite (HWS) (Fig. 3). The hanging wall zone, situated 'stratigraphically' above the hanging wall serpentinite, consists of metapyroxenites, metagabbros and rodingites. A typical borehole profile (Fig. 4), cross-cutting a major portion of the central part of the Msauli

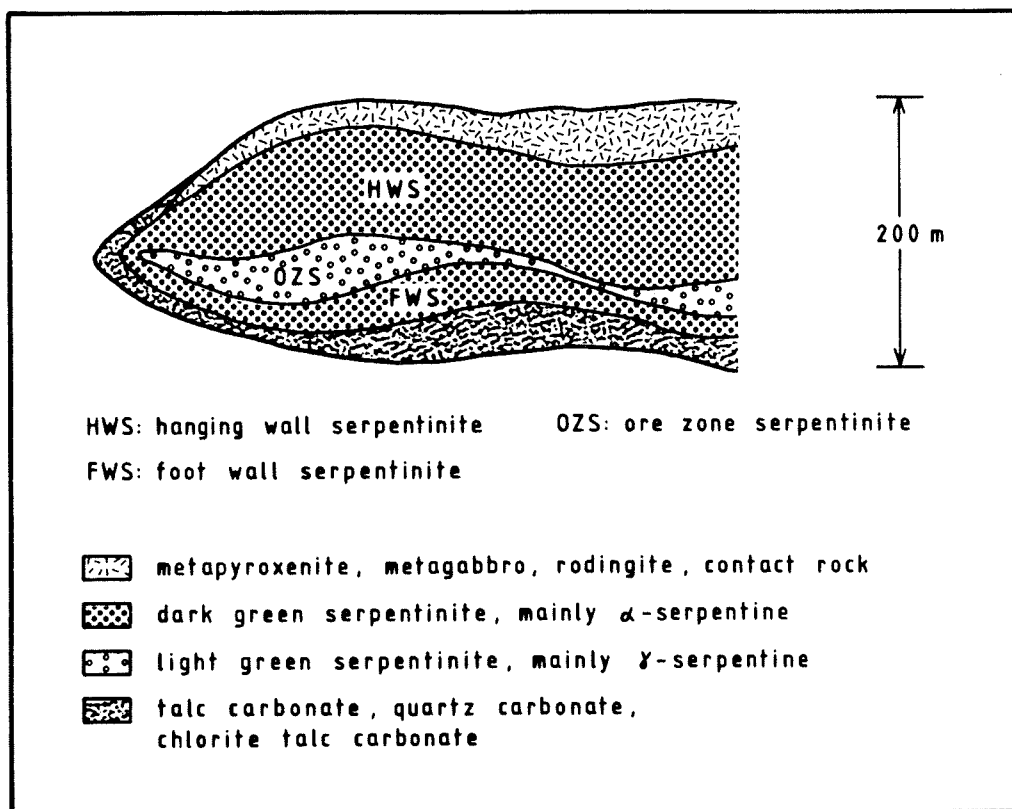


Figure 3 : Schematic cross-section of the Msauli ultramafic body.

intrusion, depicts in greater detail the rock types encountered west to east across the ultramafic body as well as sample localities of core taken for further petrological and geochemical studies.

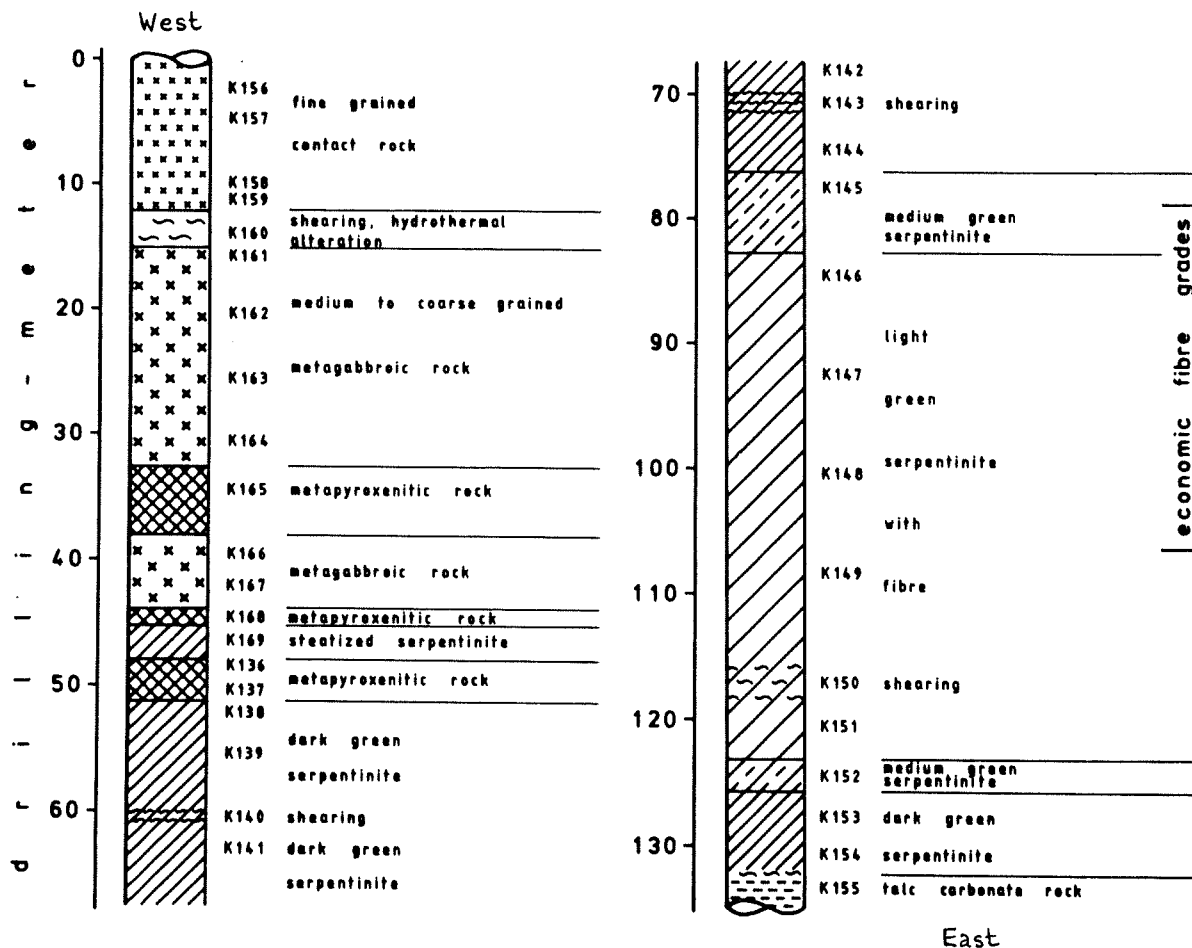


Figure 4 : Borehole profile across the central part of the Msauli ultramafic body (Office-section, K-level, borehole OK 7) showing the localities of core samples studied.

A. Serpentinites

1. Lithology

The larger part of the Msauli intrusion consists of serpentinites which are enveloped by the rocks of the footwall alteration zone and the hanging wall zone. Where unweathered the serpentinites are coloured in various shades of green. The OZS typically has a light grass-green colour while the FWS and HWS, in contrast, are medium-to-dark green. In the 'stratigraphically' uppermost parts of the HWS (east) the serpentinite is almost black, due partly to an increase in the amount of fine-grained accessory chromite present in the rocks. Furthermore, the FWS, and in particular the HWS, appear to be much more competent and massive than the OZS.

The dunite from which the serpentinites were derived possessed a distinct cumulus texture. The euhedral olivine grains are now completely serpentinized to olivine pseudomorphs which range in size from 0,5 to 2 mm but are locally up to 6 mm in diameter.

In the serpentinites two types of veins can be observed: (i) magnesite veins, and (ii) cross-fibre chrysotile veins, which form asbestos. Magnesite veins predominate in the FWS and HWS, while cross-fibre chrysotile veins predominate in the OZS. In most cases the magnesite veins are younger than the cross-fibre veins. The cross-fibre veins which form an economically exploitable stockwork are strongly concentrated towards the OZS, whereas the FWS and HWS are generally devoid of economic quantities of cross-fibre. Depending upon their thickness the cross-fibre veins in the OZS generally measure up to 20 cm in length. Most veins have a thickness of between 2 and 8 mm but in high grade areas they may be 20 mm thick.

Accessory minerals found in the serpentinites, and which are visible with the unaided eye, include magnetite and chromite. In the OZS magnetite is usually concentrated either along the side walls of the cross-fibre veins, or sometimes in small clots disseminated throughout the OZS. In the FWS and HWS the magnetite occurs rather finely dispersed and hardly recognizable without optical aid. Chromite, although relatively abundant in the serpentinites, is difficult to identify macroscopically because of its resemblance to magnetite. Another accessory mineral commonly found in the FWS, and to a lesser degree in the OZS and the HWS, is magnesite, which becomes progressively abundant towards the footwall alteration zone. Apart from vein fillings magnesite occurs in small irregular patches, replacing serpentine minerals. As a rare constituent native copper was found in the OZS and in slightly weathered HWS. In the OZS the native copper occurs on slickensides as a very thin coating. A similar coating was found on fracture planes in partly disintegrated, black HWS. The copper probably results from secondary alteration processes and is not regarded as a primary mineral of the Msauli ultramafics.

2. Mineralogy

Over one hundred serpentinite samples from all parts of the Msauli ultramafic body were collected for mineralogical investigation. Some of the samples were obtained from drill core (Fig. 4), the remainder being collected from underground exposures.

X-ray diffraction studies assisted with the identification of the serpentine species. The X-ray diffraction procedures applied were described by Büttner and Saager (1982b), Whittaker and Zussman (1956) and Wicks (1979). Using these methods it was found that the most common serpentine mineral is lizardite, followed by chrysotile $2M_{C1}$, chrysotile $20rc_1$, and antigorite. The distribution of lizardite and chrysotile in the borehole section depicted in Fig. 4 was determined by Büttner and Saager (1982b) by means of quantitative XRD, using the $^{008}_{chr}/^{204}_{liz}$ reflections. These authors found that the chrysotile content in the FWS and HWS usually does not exceed 5 per cent. A considerable increase in the chrysotile content occurs towards the OZS, where the total chrysotile content rises to approximately 35 per cent. Slip-fibre chrysotile, occurring in shear zones of the FWS may also give rise to local, uneconomic enrichments in chrysotile.

Using the X-ray technique described by Wicks (1979), the cross-fibre chrysotile was identified as chrysotile $2M_{C1}$ (Büttner, 1983a). Further powder diffraction studies on homogeneous serpentinite samples and on separated olivine pseudomorphs showed that chrysotile $20rc_1$ in the OZS occurs as a minor constituent in addition to lizardite and chrysotile $2M_{C1}$. Antigorite is restricted to some shear zones, where it probably formed under elevated

stress conditions. Thus, antigorite cannot be regarded as a characteristic serpentine mineral of the Msauli serpentinites. Typical X-ray diffraction charts, obtained from samples of the FWS, OZS and HWS are shown in Fig. 5. These charts clearly depict the differences in mineralogy between the three types of serpentinite.

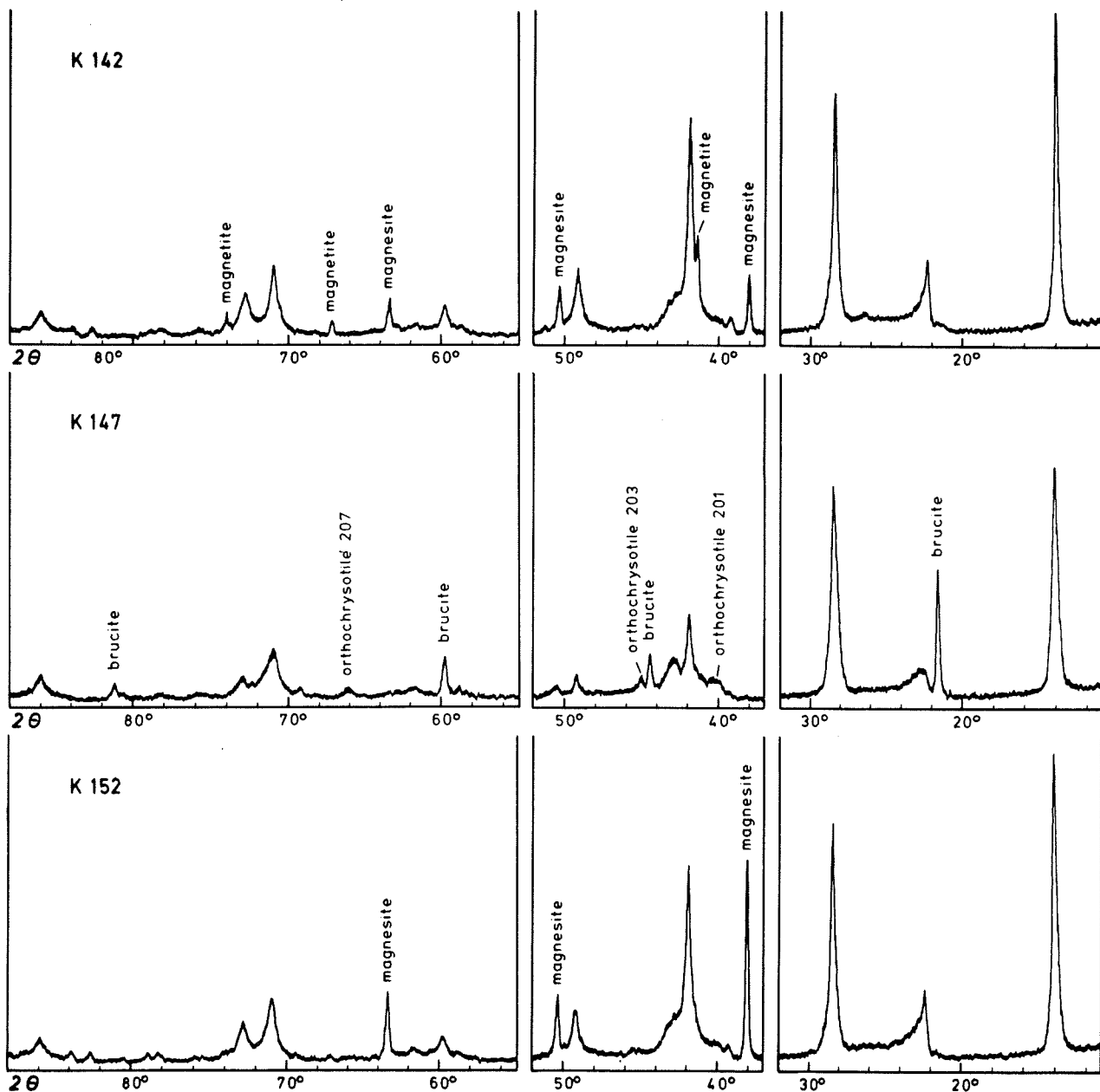


Figure 5 : Characteristic X-ray diffraction charts of FWS, OZS, and HWS samples.

K 142 (HWS): lizardite, magnesite, magnetite, and traces of chrysotile.

K 147 (OZS): lizardite, chrysotile 2Mc₁, chrysotile 20r_{c1}, and brucite.

K 152 (FWS): lizardite, magnesite, and traces of chrysotile.

Thin section studies of samples from all parts of the serpentinite zone revealed that lizardite in olivine pseudomorphs typically displays a pseudofibrous habit. According to Cressey (1979), Prichard (1979) and Wicks and Zussman (1977), such pseudofibres, which are sometimes called 'apparent fibres', are a result of parallel stacking of tiny lizardite plates. Depending upon their optical properties, two types of lizardite pseudofibres can be distinguished. Tertsch (1922) first described them as α - and γ -serpentine according to the orientation of the fibre axes, either parallel $n\alpha$ (α -serpentine), or parallel $n\gamma$ (γ -serpentine). In the Msauli serpentinites, γ -serpentine forms relatively coarse, and in thin section, colourless pseudofibres, while α -serpentine forms rather fine and wavy pseudofibres, which have a light yellow-green colour.

X-ray diffraction studies of separated olivine pseudomorphs from the OZS showed that chrysotile 20rc1 occurs in small quantities in addition to lizardite in these olivine pseudomorphs. However, since chrysotile also forms γ -serpentine both serpentine types are virtually indistinguishable in olivine pseudomorphs by thin section study alone. Most serpentinite samples investigated possess both, α - and γ -serpentine pseudofibres in olivine pseudomorphs. Only the 'stratigraphically' uppermost parts of the HWS are formed by olivine pseudomorphs that consist almost exclusively of α -serpentine lizardite. Generally, the γ -serpentine, when present in olivine pseudomorphs, is restricted to their cores, rimmed by α -serpentine (Fig. 6). Textures resulting from this arrangement resemble either mesh or hourglass textures, but also a combination of both. Mesh textures are formed when the cores of olivine pseudomorphs, which consist of either orientated or unorientated γ -serpentine, are thinly rimmed by radially orientated α -serpentine. Hourglass textures result when olivine grains are completely replaced by orientated α -serpentine, and also when the cores are replaced by orientated γ -serpentine. The latter type of γ -serpentine hourglass textures are found in the OZS, while α -serpentine hourglass textures occur mainly in the 'stratigraphically' uppermost parts of the HWS. In places, however, original mesh and hourglass textures have been obliterated by tectonic deformation which produced a subparallel alignment of former α -serpentine rims over distances exceeding 20-30 mm.

The spatial distribution of the principal textural types, as observed in the serpentinites of the Msauli ultramafic body, is shown in Fig. 7. The microscopically observed distribution of the two types of pseudofibres, i.e. γ -serpentine in the cores of the olivine pseudomorphs and α -serpentine around their rims, coincides with the macroscopic observation that γ -serpentine is enriched in the central zone of the Msauli ultramafic body (OZS) while α -serpentine is enriched in its outer zones (FWS and HWS). The genetic implications of this observation will be discussed later.

The chrysotile fibres in cross-fibre veins generally form at right angles to the sidewalls of the veins, although there may be sections of bent veins where the fibre axes possess oblique angles to the sidewalls. However, considering the entire length of individual veins, the average angle between the sidewalls and the fibres is always very close to 90°. Apart from the larger cross-fibre veins, visible without optical aid and yielding economic fibre grades, numerous microveins occur throughout the OZS. They usually have a length of less than one millimetre and contain fibres some hundredth of a millimetre long. These short fibres contribute largely to the chrysotile content in the mill tailings, and have only limited economic value.

Figure 6 : Photomicrographs of the Msauli serpentinites.

A. FWS, olivine pseudomorphs consisting of hour-glass-textured γ -serpentine surrounded by α -serpentine.

B. OZS, olivine pseudomorph consisting of γ -serpentine and brucite (light grey to white) surrounded by a small rim of α -serpentine.

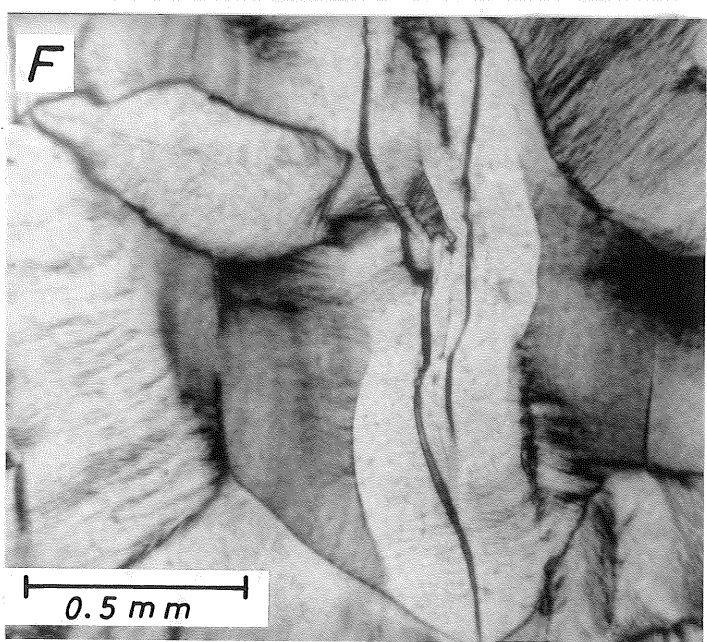
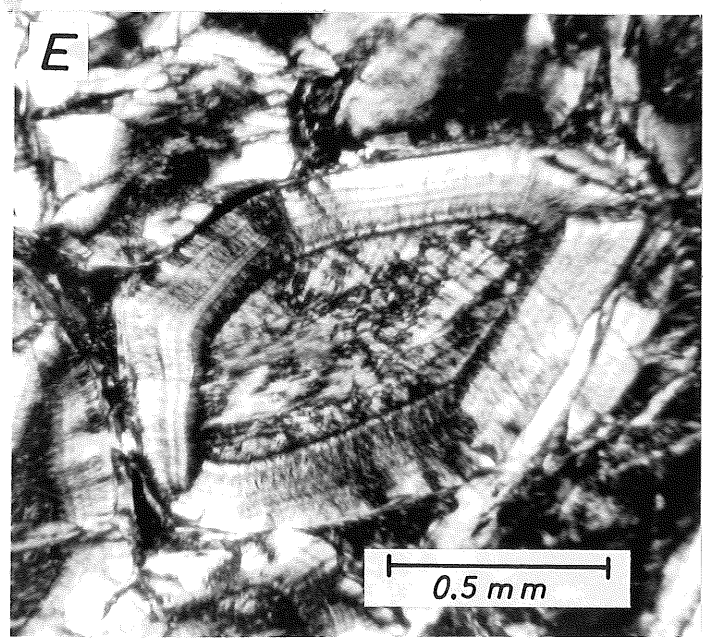
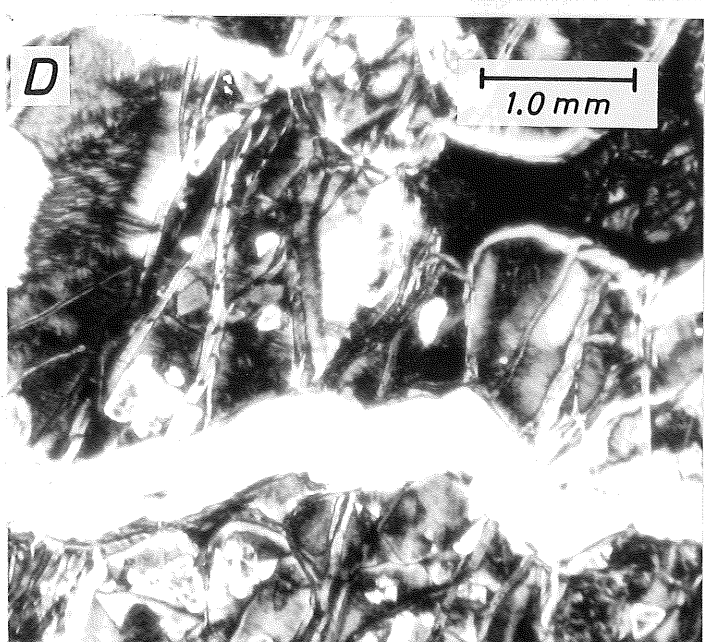
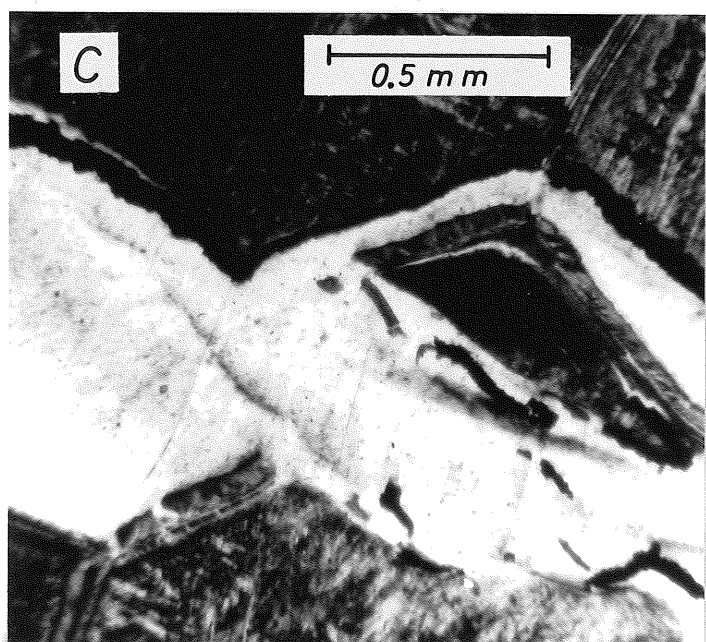
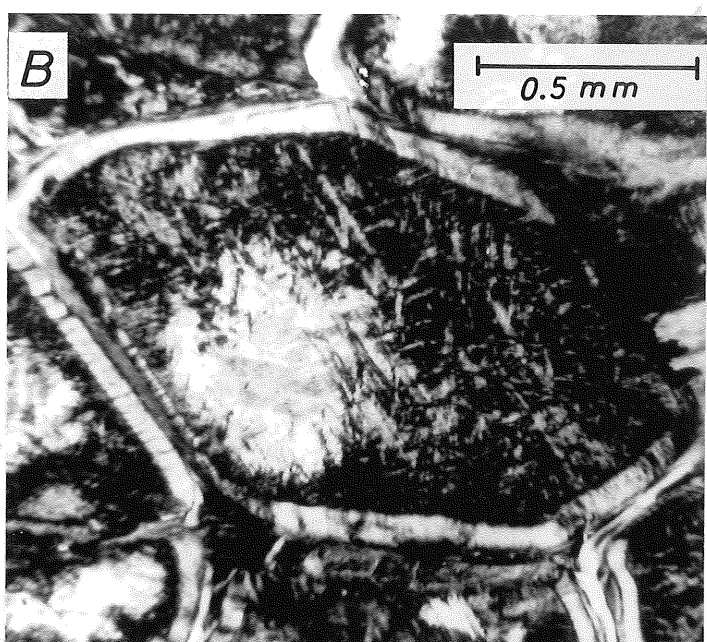
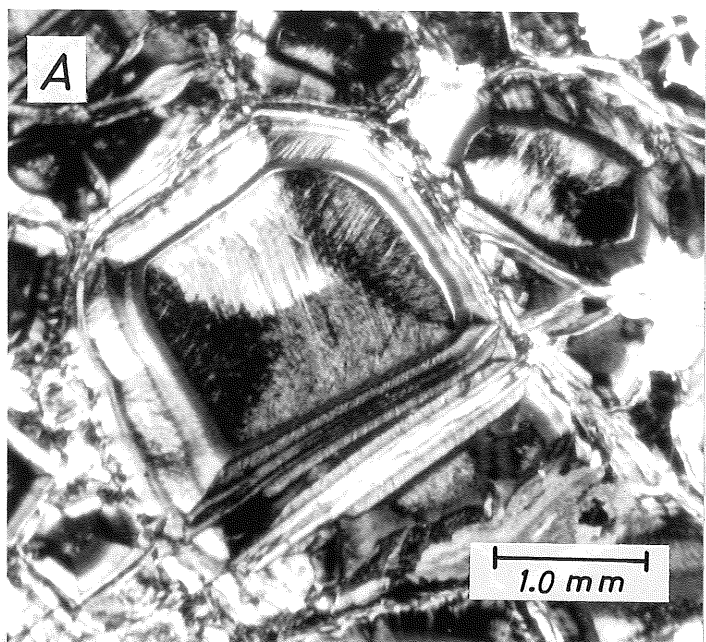
C. OZS, part of a chrysotile cross-fibre vein with magnetite seam (black) at the upper sidewall.

D. OZS, mesh-textured serpentinite consisting largely of γ -serpentine, some α -serpentine and brucite (white specks). A chrysotile cross-fibre vein with perfectly matching opposing sidewalls is also present.

E. HWS, olivine pseudomorph consisting of an inner core formed by γ -serpentine (partly unorientated) and an outer rim formed by α -serpentine.

F. HWS, hourglass-textured α -serpentine and chromite grain (lower part of photograph).

All photomicrographs were taken with crossed polarized light.



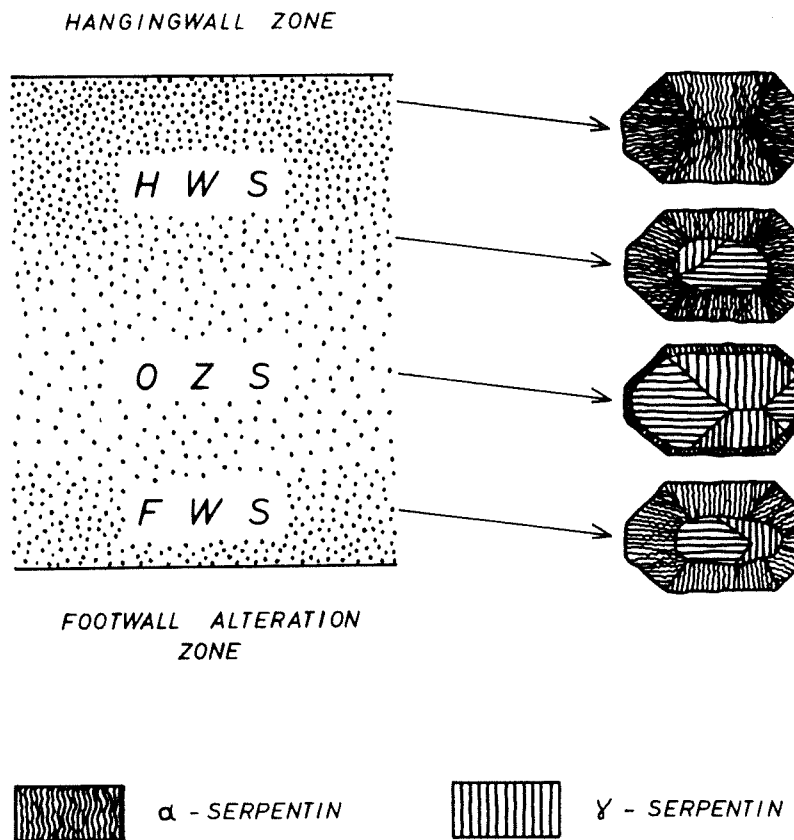


Figure 7 : Schematic representation of the spacial distribution of serpentine textures.

Often a concentration of minute magnetite crystals is found in small seams orientated parallel to the sidewalls of the chrysotile cross-fibre veins. Usually, these seams occur as a parting between the cross-fibre in the veins and their sidewalls (Fig. 6C). In most cases the interiors of the cross-fibre veins are devoid of magnetite with only the very large and wide veins in places possessing a median suture, the latter accentuated by a thin magnetite seam. The total magnetite content in the OZS is lower than in the HWS, and the identification of magnetite in bulk samples by means of X-ray diffraction was only possible in samples from the HWS.

Further opaque or semiopaque minerals found in the Msauli serpentinites include chromite and heazlewoodite. Chromite is a frequent accessory mineral in the HWS, but is less common in the FWS. Surprisingly little chromite occurs in the OZS. Relics of former chromite grains indicate, however, that original chromite grains in the OZS have been largely replaced by magnetite, serpentine and chlorite. The chromite occurring in the FWS and HWS characteristically shows a dark reddish-brown colour and subhedral forms in thin section. The size of individual chromite grains varies between 0,1 and 0,5 mm with the larger grains being concentrated in the FWS. Along cracks and on grain boundaries the chromites are replaced by magnetite. Heazlewoodite was found only in minute quantities in the OZS. Typically, it has anhedral, roundish forms and grain sizes of about 0,2 mm. Under the ore microscope the heazlewoodite is white with a weak yellow tint and it has a high reflection and weak anisotropism. The microscopic identification of the heazlewoodite was confirmed by electron microprobe analysis (Büttner, 1983a).

A further accessory mineral in the Msauli serpentinites is chlorite. It has a fibrous habit and occurs interstitially between the olivine pseudomorphs, often associated with magnetite. In thin section, the chlorite is almost colourless, but displays anomalous bluish, and sometimes brownish interference colours. According to X-ray diffraction studies, using criteria given by Albee (1962), Brindley and Gillerey (1956), Hey (1954), and Wetzel (1973), the chlorite is a Mg-rich and Al-poor variety belonging to the pennine-chlinochlor series. Subsequent electron microprobe analysis confirmed these findings (Büttner, 1983a). Chlorite is often associated with altered tremolitic material, which has been partly replaced by chlorite. This suggests that chlorite is not a primary mineral in the serpentinitized dunites but most likely originated from a pyroxene (diopside) which first altered to tremolite and then subsequently to chlorite.

Noticeable amounts of magnesite were determined by X-ray diffraction analyses of bulk samples of the FWS and the HWS (Table I). Most of the magnesite in the HWS is related to veins and shear zones, while in the FWS magnesite replaces serpentine in olivine pseudomorphs. The magnesite content increases strongly towards the footwall alteration zone.

A relatively widespread secondary mineral in the OZS is brucite. Although the brucite content varies from place to place, its average concentration is estimated to be some 10 per cent. A sharp drop in the brucite content occurs towards both the FWS and the HWS. In thin section the brucite is easily identified by its anomalous brownish interference colours. Brucite enrichment usually occurs in the centres of olivine pseudomorphs where it forms fibres which are intimately intergrown with the γ -serpentine.

B. Footwall Alteration Zone

The gradual increase in the magnesite content in the FWS (approaching the footwall alteration zone) leads to transitional magnesite-rich serpentinites and the appearance of talc in talc-carbonate rocks, the latter usually being devoid of any serpentine minerals. The talc-carbonate rocks are readily identified on surface or in underground exposures by their light greyish colouration, together with their softness and physical incompetence. Carbonate and talc occur in almost equal proportions in the talc-carbonate rocks and the magnesite is sometimes replaced by dolomite or, in rare cases, by calcite. These carbonate minerals usually occur in the form of rhombohedrons which are enveloped by talc flakes. The existence of pseudomorphosed cross-fibre veins in the talc-carbonate rocks indicates that steatization of the original serpentinite took place after the formation of the cross-fibre veins.

Common accessory minerals in the talc-carbonate rocks include chromite, magnetite and chlorite. The optical properties of the chromites in the talc-carbonate rocks are identical to those found in the serpentinites, but in the talc-carbonate hosts the chromites are strongly corroded and fractured. They are usually enveloped by purplish-brown chlorite, which in thin section is only weakly coloured, with a very low birefringence. According to X-ray diffraction studies this chlorite is a Cr-and Mg-rich variety, but is not kaemmererite. A second chlorite variety occurring in the talc-carbonate rocks has optical properties which are identical to those of the chlorites found in the serpentinites. The magnetite in the talc-carbonate rocks forms small aggregates similar to the magnetite aggregates in the serpentinites.

TABLE I

MINERAL DISTRIBUTION ALONG BOREHOLE OK7 PROFILE,
K-LEVEL, OFFICE SECTION, MSAULI MINE

	QUARTZ	ALBITE	MUSCOVITE	TREMOLITE	CALCITE	DOLOMITE	MAGNESITE	CHLORITE	TALC	BRUCITE	CHRYSOTILE	LIZARDITE	ANTIGORITE	MAGNETITE
K 156	XX	XXX	X		XXX			XXX	XX					
K 157	XXX	XX	X		XXX			XXX	X					
K 158	XXX	XXX	X	X	XXX			XXX	XXX					
K 159	X	XX	XX	XXX				XXX						
K 160	XXX	XX	XX	XX	XXX									
K 161	XXX	XX	XX	XXX				XXX						
K 162	XXX	XX	XX	X				XX						
K 163		XX	X	XXX				XXX						
K 164		XXX		XXX	X			X						
K 165				XXX	X			XXX						
K 166		XXX		XX				XXX						
K 167		XXX	XX	XX	XXX			XXX						
K 168				XXX				XX						
K 169					XX		X	XXX			XXX			
K 136				XXX				XXX						
K 137				XXX				XXX						
K 138					XXX			XX			XXX		X	
K 139				X	XXX			XXX			XX		X	
K 140						XX					XXX		X	
K 141						XXX						XXX	X	
K 142						XX	X				XXX		X	
K 143					XXX	X				XXX	XXX			
K 144						XX					XXX		X	
K 145						XX					XX	XXX		
K 146						X			XX	XX	XXX			
K 147						X			XX	XXX	XXX			
K 148									XX	XXX	XXX			
K 149									XX	X	XXX			
K 150						XX			X		XXX			
K 151						XXX				X	XXX			
K 152						XXX					XXX			
K 153						XX		X			XXX			
K 154						XXX						XX	X	
K 155						XXX	XX	XXX						

Data obtained by X-ray diffraction analyses
 X = trace mineral XX = minor mineral XXX = major mineral

Increased quantities of Mg-Fe-chlorite, dolomite and calcite distinguish the chlorite-talc-carbonate rocks from the talc-carbonate rocks. Additional fine-grained accessory minerals like graphite, magnetite, and sulphide minerals are responsible for the dark, sometimes black colouration of the chlorite-talc-carbonate rocks. An analysis of the HCl-insoluble residue of a typical chlorite-talc-carbonate rock sample yielded 0,16 wt per cent carbon. In samples from tectonically undisturbed areas the graphite flakes are arranged in a manner similar to the mesh textures found in the serpentinites. Chromite grains which are usually enveloped by secondary Cr-Mg-chlorite are identical to those occurring in the serpentinites and the talc-carbonate rocks. The existence of chromite, in addition to the mesh-like textures, indicates that the chlorite-talc-carbonate rocks are alteration products of serpentinites. Similar rock types, generally termed *blackwall*, are described from many other serpentinite zones throughout the world (Chidester, 1962; Hess, 1933; Sanford, 1982). At Msauli, the chlorite-talc-carbonate rocks are usually confined to a zone between the talc-carbonate rocks and the footwall country rocks. This relationship, however, is sometimes tectonically disturbed so that chlorite-talc-carbonate rocks occur in tectonic contact with the FWS.

A third rock type forming part of the footwall alteration zone is a quartz-carbonate rock. In contrast to the other two rock types of the footwall alteration zone the quartz-carbonate rocks are massive and competent, and appear largely unaffected by tectonic deformation. Approximately equal proportions of quartz and carbonate in these rocks are considered responsible for the competent behaviour of the quartz-carbonate rocks. Magnesite, followed by dolomite, are the main carbonate minerals in the quartz-carbonate rocks. The carbonates occur in the form of rhombohedrons, usually 50 to 100 microns in size, set in a matrix consisting of anhedral quartz. Accessory minerals in the quartz-carbonate rocks are chromite, fuchsite and magnetite. As in the other rock types of the footwall alteration zone, chromite occurs in the form of subhedral grains ranging between 0,1 and 0,8 mm in diameter and showing replacement around the grain margins by magnetite. Bright green fuchsite is a characteristic component of the quartz-carbonate rocks and is found preferably around chromite grains.

Underground mapping in the Msauli Mine (Büttner, 1983a) revealed that the quartz-carbonate rocks are generally surrounded by talc-carbonate rocks or, in some places, by chlorite-talc-carbonate rocks. The quartz-carbonate rocks do not occur in contact with the country rocks and a gradual transition from talc-carbonate rocks to quartz-carbonate rocks appears to be a general rule. These features, in addition to the presence of chromite, suggest that the quartz-carbonate rocks are also alteration products of serpentinites.

C. Hanging Wall Zone

Relatively poor exposures of the hanging wall zone exist in the Msauli Mine. This is related to the mining method which dictates that mining development takes place mainly in the serpentinites and in the footwall alteration zone. Hence, most rock samples examined from the hanging wall zone consist of drill cores, there being only a few underground exposures available for sampling.

As shown in Figs. 3 and 4 the HWS is 'stratigraphically' overlain by the hanging wall zone which consists of metapyroxenites, metagabbros and rodingites. The contacts between the HWS and the overlying metapyroxenites

are generally marked by a small chlorite-rich transition zone, a few centimetres wide. In most cases these contacts are tectonically undisturbed and are regarded as being of magmatic origin. The metagabbros, where unaltered, have a massive dark grey and medium-to coarse-grained appearance. Frequently, large pyroxene pseudomorphs, that are in places more than one centimeter long, are clearly visible without optical aid. Thin section and X-ray diffraction studies revealed that the original pyroxenes are now completely replaced by fibrous tremolite-actinolite intergrown with some fine-grained chlorite. The mineral assemblage now present suggests that the original pyroxenites consisted chiefly of clinopyroxenes which had a diopsidic to salitic composition (Tröger, 1969). No signs of former orthopyroxene exsolution lamella were found. Accessory minerals noted in the metapyroxenites include calcite, albite, sericite, biotite and quartz but these are usually very fine grained and difficult to identify without X-ray diffraction.

The metagabbros are mineralogically and texturally similar to the metapyroxenites but, in addition to uralitized pyroxenes, they also contain noticeable amounts of albited plagioclase. Where fresh the metagabbros form massive light greenish-grey to dark-grey coloured rocks, depending upon the contents of albite and light coloured tremolite. Usually, the metagabbros are 'stratigraphically' underlain by the metapyroxenites, but they also occur interlayered in the metapyroxenites and are in places in direct contact with the HWS. In most cases the metagabbros and metapyroxenites display magmatic contacts with the HWS. In places, however, shear zones, resulting from tectonic activity, have obliterated the original contacts. Thin section study shows that the original pyroxenes in the metagabbros are completely replaced by fibrous actinolite, tremolite and minor chlorite. Larger ophitic pyroxene pseudomorphs often contain inclusions of albited plagioclase. In other samples, albited plagioclases, several millimeters in size, occur in anhedral forms intergrown with uralitized pyroxenes of similar size. The albited plagioclases have in places been further altered to sericite or calcite. Other accessory minerals include small apatite prisms which form ubiquitous inclusions in the plagioclases, and sphene which forms euhedral crystals up to 0,5 mm in size. Quartz commonly fills fractures in the metagabbros.

The 'stratigraphically' uppermost zone of the Msauli ultramafic body consists mainly of "spinifex- and bird-track-textured" metagabbros. Both textural types are formed by acicular pyroxene pseudomorphs which consist of chlorite and talc. They are set in a fine-grained matrix consisting of tremolite, albite, chlorite, quartz, sericite and talc. The pyroxene pseudomorphs of the spinifex-textured metagabbros are arranged subparallel and vertically and are up to 15 cm long. In the bird-track-textured zone, which lies 'stratigraphically' above the spinifex zone, the pyroxene pseudomorphs are rather stubby and randomly arranged. Rock types with identical textures are known from many other Archaean ultramafic and mafic bodies and lava flows (Arndt *et al.*, 1977; Brooks and Hart, 1974; Pyke *et al.*, 1973; Viljoen and Viljoen, 1969b) and are usually explained by rapid cooling of a magmatic melt and rapid crystal growth rates (Lofgren and Donaldson, 1975; Lofgren, 1983). This comparison suggests that the spinifex- and bird-track-textured metabasalts represent the marginal zone of the Msauli ultramafic body, in which rapid cooling took place.

Rodingites form only a small part of the Msauli ultramafic body yet they are conspicuous due to their white or light greyish-green colour and coarse-grained mineral assemblage. Commonly, the rodingites occur in

irregular masses, spacially associated with the metagabbros. At one locality (Office Section, K-level) a small rodingite pod was found separated from the HWS by a 2 cm-wide contact zone rich in chlorite and clinzoisite. Petrographic and X-ray diffraction studies showed that the rodingites are composed chiefly of tremolite, grossular, diopside, idiomarble, clinzoisite, epidote and chlorite. Intergrowths of grossular and idiomarble often form pseudomorphs after plagioclase, while tremolite, diopside and chlorite form pseudomorphs after pyroxene. Clinzoisite occurs interstitially between the pseudomorphs, but also as secondary euhedral crystals. In places the clinzoisite has a pinkish colour, due to traces of manganese. Epidote occurs in accessory amounts in the form of small euhedral crystals developed in cavities. A transitional relationship between the metagabbros and the rodingites, indicated by the existence of partly rodingitized metagabbros, suggests that the rodingites constitute metasomatic replacement products of former gabbroic rocks (see also Anhaeusser, 1979).

D. Chemistry

1. Serpentine Chemistry

Electron microprobe analyses of Si, Al, Fe, and Mg in the various serpentine species of the Msauli serpentinites were carried out on polished thin sections of samples obtained from the drill core shown in Fig. 4. The instrument used was an ARL microprobe, equipped with an energy dispersive KEVEX system. Instrumental conditions were as follows: accelerating voltage 15 kV, filament current 50 μ A, probe current 15 nA, irradiation time 100 seconds. All raw data obtained were corrected for background, atomic number, absorption and fluorescence effects. A homogeneous serpentine specimen, previously analysed by means of XRF, was used as a standard. Uncertainties (2σ), obtained from 34 replicate measurements of the serpentine standard, are as follows: $\text{SiO}_2 \pm 3$ per cent, $\text{Al}_2\text{O}_3 \pm 4$ per cent, $\text{FeO}^* \pm 6$ per cent, and $\text{MgO} \pm 1$ per cent. All analyses were done in duplicate or triplicate. The difference between the total of the determined oxides and 100 per cent were attributed to H_2O .

According to the optical features of the respective serpentine minerals the analytical data were ordered into 5 distinct groups: (1) α -serpentine in olivine pseudomorphs, (2) γ -serpentine in olivine pseudomorphs, (3) cross-fibre chrysotile, (4) unorientated γ -serpentine in the centres of olivine pseudomorphs, and (5) small domains of α -serpentine between γ -serpentine pseudofibres. Table II shows the results of the microprobe analyses in these 5 groups. A graphical display of the analytical data is given in the FeO^* - SiO_2 - MgO diagram in Fig. 8. This diagram does not account for the Al_2O_3 contents of the serpentines. As a consequence, most of the data points in Fig. 9 plot below the connecting line between Fe-serpentine and Mg-serpentine, because Al is expected to partly replace Si in the serpentine lattice (Wicks, 1979). From Fig. 8 it is evident that the various serpentine species have different chemical compositions. Thus, the α -serpentine of group (1) is readily distinguished from the γ -serpentine of group (2) by the higher FeO^* and lower MgO contents of the former. The α -serpentine of group (1) also generally contains the highest Al_2O_3 contents (Table II). The α -serpentine which is darker coloured than the γ -serpentine has a relatively high FeO^* content (FeO^* denotes total iron as FeO).

In order to evaluate the interrelationships between the analysed elements of the two most widely distributed serpentine species, namely α -serpentine (group 1) and γ -serpentine (group 2), their correlation

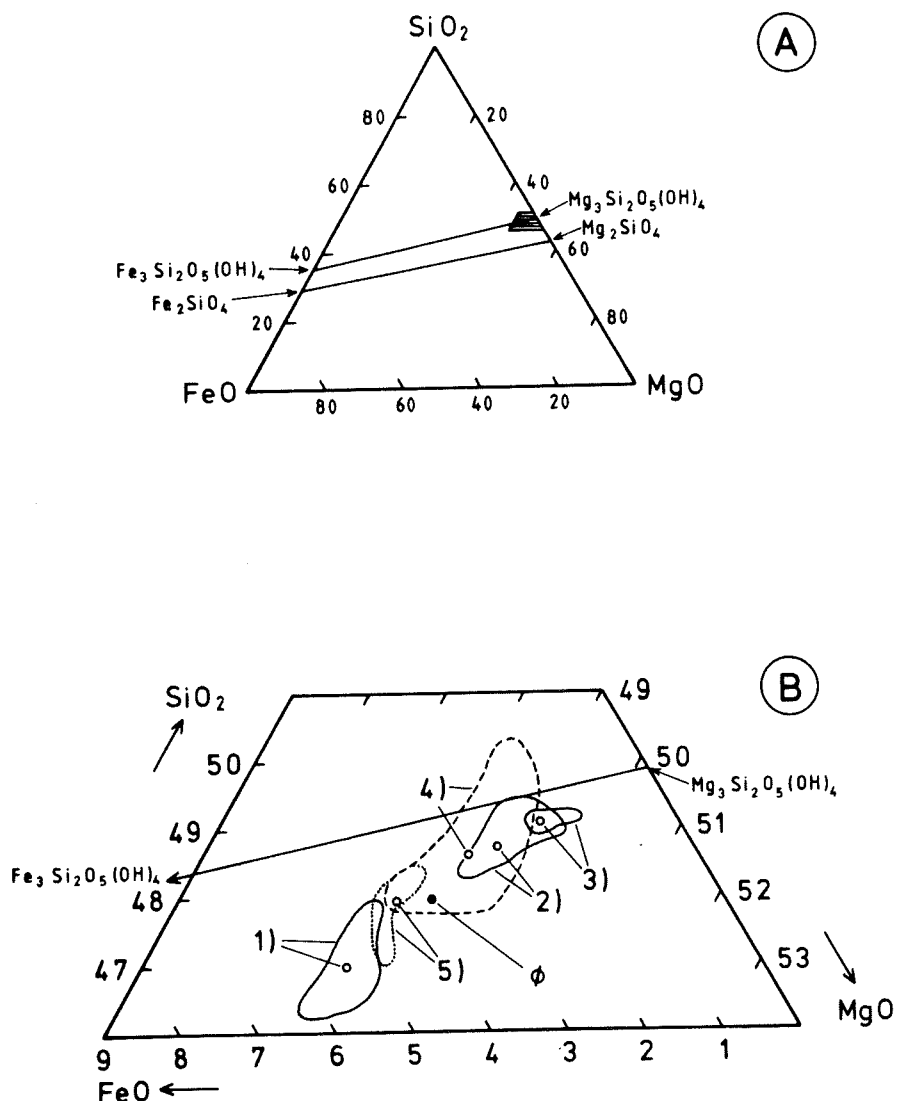


Figure 8 : $\text{FeO}^*-\text{SiO}_2-\text{MgO}$ diagram of serpentine species occurring in the Msauli serpentinites. Numbers are identical to those in Table II.

TABLE II

GROUPED AVERAGE ANALYSES AND STANDARD DEVIATIONS OF SERPENTINE
SPECIES OCCURRING IN THE MSAULI SERPENTINITES

Group	Number of samples	(1) 22	(2) 16	(3) 5	(4) 6	(5) 5
SiO ₂		38,66 ± 0,67	39,59 ± 0,53	39,81 ± 0,35	39,65 ± 1,12	39,61 ± 0,51
Al ₂ O ₃		1,02 ± 0,23	0,97 ± 0,21	0,79 ± 0,02	1,05 ± 0,20	1,12 ± 0,28
FeO*		4,43 ± 0,39	2,04 ± 0,57	1,45 ± 0,03	2,41 ± 0,91	3,49 ± 0,33
MgO		39,26 ± 0,37	39,64 ± 0,47	39,87 ± 0,43	39,53 ± 0,35	39,56 ± 0,15
H ₂ O		16,62 ± 0,91	17,76 ± 0,57	18,07 ± 0,77	17,37 ± 1,37	16,23 ± 0,32

*) Total iron expressed as FeO.

- (1) α -serpentine (2) γ -serpentine in olivine pseudomorphs (3) cross-fibre chrysotile
 (4) unorientated γ -serpentine in olivine pseudomorphs (5) domains of α -serpentine
 between γ -serpentine pseudofibres in olivine pseudomorphs.

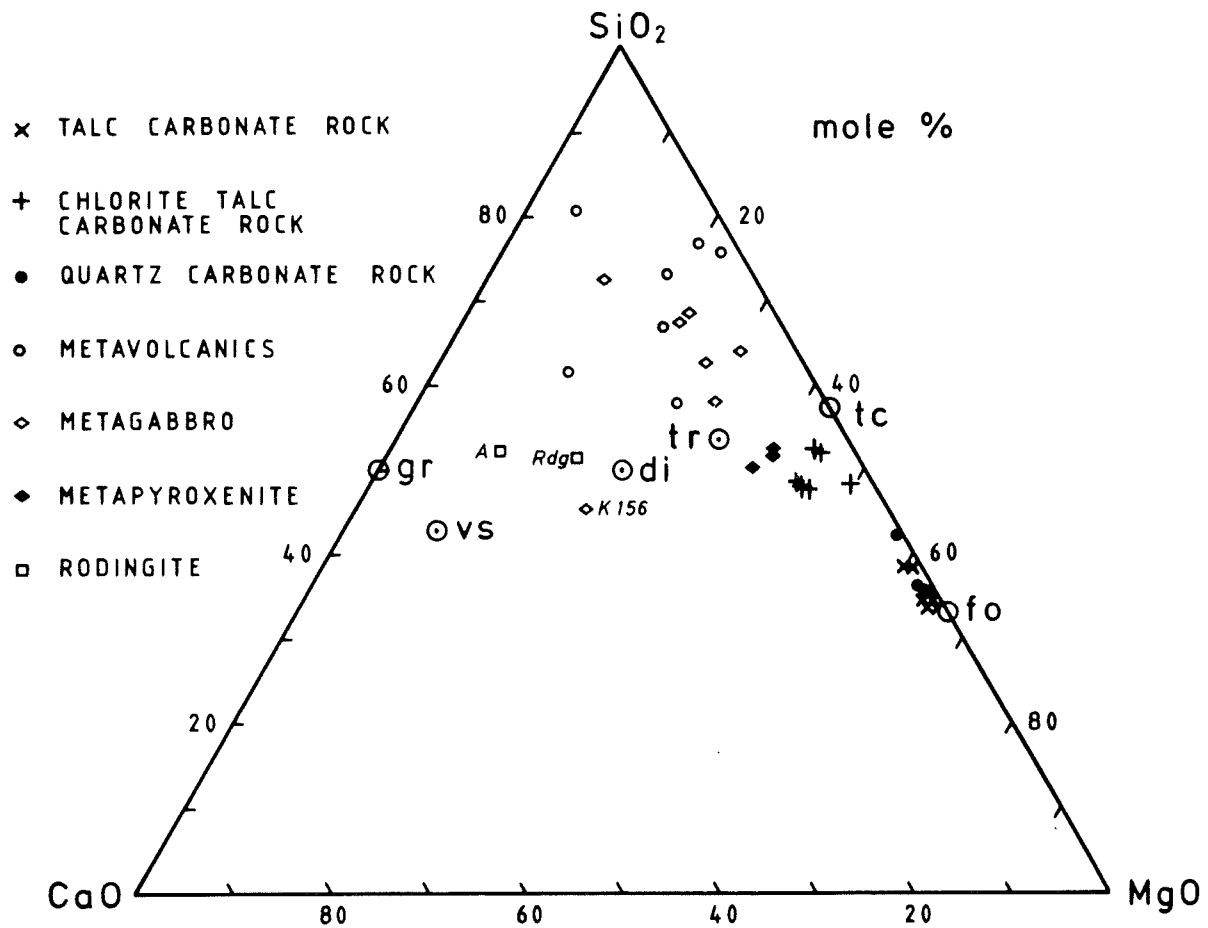


Figure 9 : $CaO-SiO_2-MgO$ diagram of the various rock types of the Msauli ultramafic body.

gr: grossularite, vs: vesuvianite (idiocrase), di: diopside, tr: tremolite, tc: talc, fo: forsterite, Rdg: rodingite composite analysis, K 156 rodingitized metagabbro.

TABLE III

MATRICES OF CORRELATION COEFFICIENTS FOR
 α -SERPENTINE (22 Samples) and γ -SERPENTINE (16 samples)

α -serpentine	SiO ₂	Al ₂ O ₃	FeO	MgO
Al ₂ O ₃	0,211			
FeO	<u>-0,585</u>	-0,351		
MgO	<u>0,795</u>	0,110	-0,234	
H ₂ O	<u>-0,860</u>	-0,306	0,190	<u>-0,917</u>
γ -serpentine	SiO ₂	Al ₂ O ₃	FeO	MgO
Al ₂ O ₃	<u>-0,632</u>			
FeO	<u>-0,870</u>	<u>0,661</u>		
MgO	0,317	-0,455	<u>-0,647</u>	
H ₂ O	-0,490	-0,018	0,107	<u>-0,755</u>

Significant values ($t_{0,99}$) are underlined.

coefficients were calculated and, as shown in Table III, elements correlating significantly are not identical for both serpentine types. A significant negative correlation coefficient between SiO_2 and Al_2O_3 , and between SiO_2 and FeO^* for γ -serpentine points towards a replacement of Si in the tetraeder position in the serpentine lattice by Al and Fe. In α -serpentine, however, Si seems to be replaced chiefly by Fe. A replacement of Mg by Fe in the octaeder position of the γ -serpentine lattice is suggested by the significantly negative correlation coefficients. The correlation coefficients between SiO_2 , MgO , and H_2O for α -serpentine indicate different degrees of hydration in the samples considered.

2. Whole Rock Geochemistry

Some 50 rock samples, largely obtained from the drill core from borehole OK7 on K-level Office Section (Fig. 4), but also from other drill cores and from underground exposures, were analysed for major and trace elements (Cr, Ni, and Cu) using standard XRF, flame photometry, and atomic absorption methods. All rock types studied in this paper are represented by at least two samples but usually by more. The mass of the original sample was generally about 1 kg. However, large samples were taken when the sample material was inhomogeneous. The analytical data was averaged and is listed in Table IV. In addition, some of the data are graphically displayed in the CSM-diagram (Fig. 9).

The three types of serpentinite are characterized by different concentrations of SiO_2 , Fe_2O_3^* , (*total Fe expressed as Fe_2O_3) MgO , and Cr. Thus, SiO_2 , Fe_2O_3^* , and Cr show increasing trends from the FWS to the OZS and to the HWS, while MgO has a maximum in the OZS and a minimum in the HWS. These trends are consistent with those generally observed in differentiated ultramafic intrusions and in Archaean ultramafic lava flows (Arndt *et al.*, 1977; Beswick, 1983; Viljoen and Viljoen, 1970; Williams and Hallberg, 1973). If recalculated water free, the chemical composition of all three serpentinite types is dunitic and, in terms of the CMS-system (Fig. 9), the serpentinites approach the composition of forsterite.

The metapyroxenites and metagabbros differ from the serpentinites in respect of SiO_2 , Al_2O_3 , Fe_2O_3^* , MnO and CaO which are lower in the serpentinites, and in respect of MgO , Cr, and Ni which are higher in the serpentinites. The volatile contents (mainly water) are generally lower in the rocks of the hanging wall zone than in the serpentinites. The metagabbros differ from the metapyroxenites mainly by lower MgO and higher SiO_2 , Al_2O_3 , and TiO_2 contents. However, both the metapyroxenites and the metagabbros possess unusually high MgO -contents compared with typical clinopyroxenites (wehrlites) and gabbros, respectively (LeMaitre, 1976). The rodingites are chemically similar to the metagabbros but have considerably higher CaO contents.

The rocks of the footwall alteration zone are comparable to the serpentinites in respect of their SiO_2 contents. Major gains or losses were, however, recorded for most of the other major oxide elements in the rocks of the footwall alteration zone, with the chlorite-talc-carbonate rocks registering the greatest changes.

IV. DISCUSSION

Mineralogical, geochemical, textural, and structural features provide ample evidence for a magmatic origin for the Msauli ultramafic intrusion. These features suggest that an ultrabasic magma, consisting of a melt with

TABLE IV

AVERAGE ANALYSES AND STANDARD DEVIATIONS OF THE ROCK TYPES OCCURRING IN THE
MSAULI ULTRAMAFIC BODY

Rock Type	ctc	qc	tc	FWS	OZS	HWS	mpx	mgb	rdg
Number of Analyses	(9)	(3)	(8)	(6)	(9)	(7)	(3)	(3)	(1)
SiO ₂	36,40±6,72	36,94±14,03	30,00±1,69	34,01±1,31	35,84±1,34	36,47±0,81	46,39±4,21	48,44±1,94	44,09
TiO ₂	0,20±0,13	0,06±0,07	0,04±0,05	0,11±0,07	0,08±0,07	0,08±0,08	0,08±0,03	0,29±0,19	0,07
Al ₂ O ₃	4,63±2,71	1,81±0,06	1,85±0,39	1,63±0,77	1,40±0,54	1,63±0,23	7,63±2,08	14,16±4,85	13,98
Fe ₂ O ₃ *	8,68±2,99	3,03±2,58	4,96±0,47	4,48±0,67	4,53±1,05	5,58±1,13	7,33±2,16	9,08±3,47	3,81
MnO	0,15±0,03	0,10±0,03	0,13±0,03	0,11±0,02	0,08±0,02	0,10±0,02	0,13±0,03	0,13±0,02	0,14
MgO	28,81±6,14	26,37±5,98	36,30±0,75	41,82±0,57	42,42±0,92	39,84±0,86	23,94±2,18	13,53±2,92	11,28
CaO	3,12±2,01	0,55±0,25	0,65±0,33	0,18±0,14	0,05±0,05	0,10±0,16	8,04±0,84	5,68±1,50	23,02
Na ₂ O	0,14±0,19	0,04±0,06	0,04±0,06	0,07±0,05	0,05±0,05	0,05±0,04	0,07±0,03	1,79±0,39	0,32
K ₂ O	0,16±0,23	0,33±0,04	0,03±0,05	0,10±0,07	0,07±0,07	0,07±0,07	0,03±0,01	2,31±1,95	0,07
LOI	17,84±7,57	30,01±6,60	25,69±1,03	17,49±1,64	15,23±1,62	14,76±0,95	6,18±1,68	5,57±1,74	3,65
TOTAL	100,13	99,24	99,69	100,00	99,75	98,68	99,82	100,98	100,44

Cr (ppm) 1960±930 1030±110 1110±580 2130±150 2210±300 3420±1030 2740±180 1190±620 n.d.
 Ni (ppm) 1360±570 1440±410 2000±130 2390±250 2410±100 2210±150 2410±3020 310±140 n.d.
 Cu (ppm) 37±37 2,3±0,6 2,2±1,2 n.d. n.d. n.d. n.d. n.d.

ctc = chlorite-talc-carbonate rock; qc: quartz-carbonate rock; tc: talc-carbonate rock; FWS: footwall serpentinite; OZS: ore zone serpentinite; HWS: hanging wall serpentinite; mpx: metapyroxenites; mgb: metagabbros; rdg: rodingites.

n.d. = not detected

* Total iron expressed as Fe₂O₃

olivine crystals in suspension (crystal mush), differentiated under the influence of gravity. The olivine crystals settled to form a cumulate, while the interstitial melt segregated mainly upwards. The progressive crystallization of the melt resulted first in the formation of pyroxenitic rocks and later in the development of gabbroic rocks. The upper zone of the intrusion crystallized rapidly, giving rise to the formation of spinifex- and bird-track-textures.

No indication as to the time of emplacement of the ultramafic magma, with respect to the country rock, could be determined. Other ultramafic bodies occurring elsewhere in the Barberton greenstone belt are all confined to the Onverwacht Group. They are therefore regarded as magmatic intrusions or lava flows related to the Onverwacht magmatic activity (Anhaeusser, 1981b, 1983; Viljoen and Viljoen, 1969b,c, 1970). Because ultramafic rocks are absent in the Fig Tree and Moodies successions two assumptions can be made: (i) the ultramafics in the Barberton greenstone belt were not emplaced tectonically as solid intrusions from deep levels of the Archaean crust and (ii) the magmatism which led to the formation of the ultramafic rocks ceased before the onset of the deposition of the Fig Tree Group. Accepting this argument it might be further concluded that the Msauli ultramafics were emplaced contemporaneously with, or shortly after, the deposition of the Swartkoppie Formation at the top of the Onverwacht Group.

Tectonic deformation and shearing along the footwall of the Msauli ultramafic body (and which is considered to be related to the Maanhaar Fault) indicates that the present relationship between the Msauli ultramafic body and its footwall country rocks does not reflect the original stratigraphic situation. Thrusting of the Swartkoppie Formation, together with the overlying Fig Tree and Moodies groups, onto the folded Kromberg Formation also caused minor shears on the hanging wall side of the Msauli ultramafic body. Regional mapping carried out in the vicinity of the Msauli Mine (Büttner, 1983a) shows, however, that no major stratigraphic break exists on the hanging wall side of the Msauli intrusion. Hence, it is contended that the stratigraphic relationship existing between the Swartkoppie Formation and the Msauli ultramafic body has remained essentially unchanged.

Neither the surface outcrops nor the underground exposures allow the positive identification of a possible high temperature alteration aureole surrounding the Msauli intrusion. This is because the surface rocks are either highly weathered or, more often, covered by scree, while underground exposures are limited to the Msauli ultramafic body itself. It therefore still remains questionable whether the Msauli intrusive was initially emplaced into unconsolidated volcanics of the Swartkoppie Formation as a sub-sea-floor sill or, alternatively, as a submarine ultramafic lava flow, deposited in a topographic depression. In either case it is likely that hydrothermal sea water circulation played a major role during the cooling and subsequent alteration of the Msauli ultramafic rocks. Circulating hydrothermal sea water along mid-ocean ridge zones yields alteration mineral assemblages in basic and ultrabasic rocks identical to those observed in the Msauli intrusion (Hajash, 1975; Humphris and Thomson, 1978; Ito and Anderson, 1983; Liou and Ernst, 1979; Seyfried and Dibble, 1980). Thus, it is assumed that the present mineralogical composition of the Msauli ultramafics is largely a result of alteration processes similar to those which account for the alteration of mid-ocean ridge volcanic rocks.

From their spacial distribution, as well as from textural, geochemical and mineralogical features, the formation of the rodingites appears to be

linked to the formation of the metagabbros. The albitization of the plagioclases in the gabbroic rocks released large amounts of Ca, which was probably responsible for the local Ca-metasomatism which resulted in the formation of the rodingites. Wenner (1979) suggested, on the basis of hydrogen, oxygen, and carbon isotopic data, that rodingites may form during hydrothermal alteration related to sea-floor spreading. As outlined above, the alteration of the Msauli ultramafics has also been related to sea water alteration and it is thus likely that sea water circulation could have been responsible for the redistribution of the Ca which led to the formation of the rodingites.

The serpentinization of the dunitic zone of the Msauli ultramafic body appears to have taken place in two stages which can be correlated with the formation of α - and γ -serpentine. Petrographic studies of serpentinization processes have shown that the serpentinization of olivine grains generally commences at grain boundaries or along cracks, and continues towards the grain centres (Prichard, 1979; Wicks and Whittaker, 1977). This process leads to the formation of mesh textures consisting of pseudofibres which radiate around the yet unserpentinized grain centres. According to Wicks and Whittaker (1977) the serpentinization of olivines often takes place in two stages. During Stage 1 the mesh rims are formed, and during Stage 2 serpentinization of the remaining olivine takes place. The serpentinization of olivines may, however, be completed after the first stage resulting in the development of hourglass textures. Cressey (1979) argued, however, that mesh rims are a result of secondary recrystallization of entirely serpentinized olivine grains. For geochemical reasons this view seems untenable in the case of the Msauli serpentinites. As shown in Fig. 8 the α -serpentine, forming the mesh rims, deviates widely from the 'ideal serpentine' as defined by the connecting line between Fe-serpentine and Mg-serpentine. The γ -serpentine, in contrast, has a composition close to the 'ideal serpentine', and since recrystallization processes commonly yield 'purer' crystals compared to their precursors, it seems highly improbable that the α -serpentine in the mesh rims is a result of recrystallization of former γ -serpentine as found in the mesh centres.

The two types of serpentine occurring in the Msauli serpentinites, α - and γ -serpentine, respectively, must have formed under different physico-chemical conditions. It is envisaged that the formation of the α -serpentine can be correlated with the hydrothermal sea water alteration, shortly after emplacement. The circulating sea water mainly affected the HWS and FWS, and did not proceed into the OZS. The formation of γ -serpentine and the serpentinization of the OZS took place during a second stage of serpentinization, probably after the folding of the Barberton greenstone belt.

The temperatures of formation of the α -serpentine are estimated at between 315° and 500°C. These figures are in accordance with results of experimental investigations conducted by Chernosky (1973), Evans *et al.*, (1976), Johannes (1968), and Moody (1976). The paragenesis of the OZS, consisting of relatively crude γ -serpentine pseudofibres (lizardite and chrysotile 20rc1), brucite and heazlewoodite, indicates rather low serpentinization temperatures for this zone. According to Moody (1976) and Prichard (1979), large lizardite crystals, as present in the γ -serpentine pseudofibres, form preferably at temperatures below 345°C. Moody (1976) also found that brucite-bearing serpentinites that contain only small quantities of magnetite generally form at low temperatures. This applies to the OZS, because the magnetite found in these serpentinites is usually related to the formation of the cross-fibre chrysotile and not to the serpentinization of the olivines. Wenner and Taylor (1971, 1973, 1974) concluded, from oxygen and hydrogen isotopic studies, that

the serpentinization of ultramafic rocks, involving meteoric waters, commonly occurs at temperatures around 100°C. A further indication of low temperature serpentinization of the present OZS relates to the existence of heazlewoodite. According to Chamberlain (1966), Eckstrand (1975), and Ramdohr (1975), heazlewoodite forms as a typical trace mineral during the serpentinization of ultramafics and, according to Moh and Kullerud (1982), heazlewoodite forms in the temperature range between 100° and 200°C.

The process of serpentinization is stoichiometrically explained by several reactions (De Waal, 1971; Hostetler *et al.*, 1966; Turner and Verhoogen, 1960). Depending upon the reaction that takes place, either water, or water and silica has to be introduced into olivine in order to obtain serpentine, with or without accompanying brucite. Most of the reactions cause an increase in volume which may be as much as 53 per cent of the initial volume. Only the removal of high amounts of magnesia and silica in an 'open system' can prevent this volume increase.

The assumption that the serpentinization of the Msauli FWS and HWS was caused by circulating hydrothermal sea water involves an 'open system' during serpentinization at which time magnesia, and possibly silica were removed via solution. The Mg-charged hydrothermal solutions probably influenced the composition of the metapyroxenites and metagabbros. Another consequence of the 'open system' behaviour during the formation of the FWS and the HWS would result in the absence of any noticeable volume change in these rocks.

In contrast, high Mg-contents, combined with appreciable quantities of brucite, would render an 'open system' and removal of magnesium during the formation of the OZS untenable. It is more likely that the magnesium released during serpentinization precipitated as brucite and thus remained in the OZS. This, in turn, involves some volume increase during serpentinization. Indications of such a volume increase are found in the shear zones which occur near the transition zones of the FWS and HWS with the OZS. These shear zones, which show no preferred direction of movement, are best explained by internal stress caused by an increase in volume.

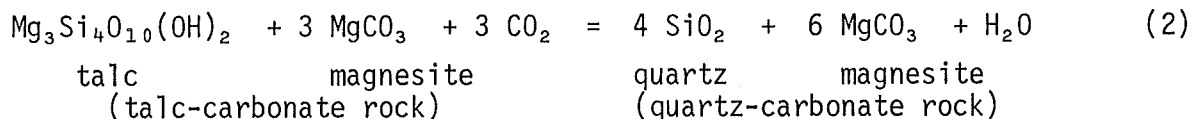
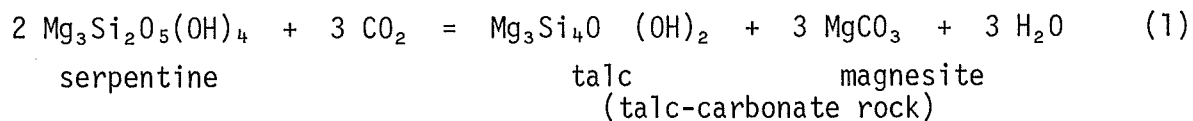
The cross-fibre chrysotile in the OZS can be related to unique stress conditions in the Msauli ultramafic body. From experimental studies it is known that chrysotile preferably grows under relatively low P/T-conditions (Moody, 1976; Yada and Iishi, 1974, 1977). It is therefore unlikely that the chrysotile fibres grew by forcing apart the sidewalls of pre-existing fractures. Fibre growth by replacement can also be excluded, since it would not explain the perfectly matching opposite sidewalls of the fibre veins. Hence, the origin of the asbestos fibre in the OZS can only be explained by antitaxial growth of chrysotile, the latter process occurring contemporaneously with the externally produced fracture dilation. Such processes, involving fibre formation, are not uncommon and occur in many environments (Ramsay, 1980). The formation of chrysotile asbestos in the Paleozoic Woodsreef serpentine in Australia by this method was explained by Glen and Butt (1981).

Solutions containing Mg, Si, and Fe, from which chrysotile could crystallize, must have been readily available in the OZS at the time of fibre formation. A likely source of these solutions is the OZS itself. The cross-fibre veins in the OZS are generally unzoned but very large veins which possess median sutures are often marked by magnetite concentrations. The general absence of zoning points, however, to a single period of fibre growth (Ramsay, 1980).

Measurements made in different parts of the Msauli Mine have shown that the asbestos cross-fibres in the OZS are orientated (Büttner, 1983a). Equal area plots (Fig. 10) indicate that fibre orientation and the Northern Porphyry are interrelated. Deformational stress, produced by the intrusion of the Northern Porphyry, caused the development and dilation of fractures in the OZS. Chrysotile fibres grew in these dilating fractures in the direction of maximum elongation, at right angles to the sidewalls (Büttner, 1983a).

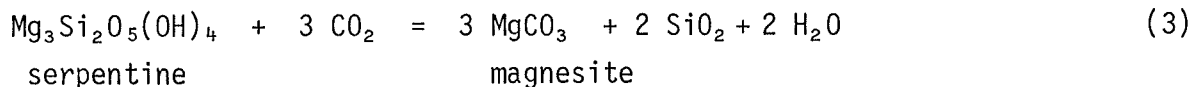
Economic cross-fibre concentrated in fractures in the more ductile OZS rather than in the more competent FWS and HWS. In addition, solutions rich in Mg, Si, and Fe were more readily available in the OZS than in other parts of the Msauli ultramafic body.

The footwall alteration zone is characterized by carbonate metasomatism that can be attributed to hydrothermal CO_2 -bearing solutions. The existence of carbonated cross-fibre veins in the talc-carbonate rocks suggests that carbonatization took place after the cross-fibre formed in the serpentinites. Reactions producing the talc-carbonate and quartz-carbonate rocks are as follows:

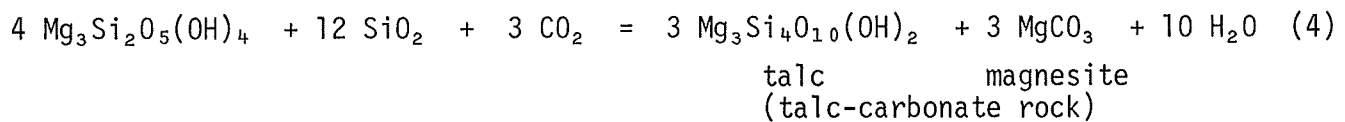


These reactions show that no additional SiO_2 is needed for the formation of the quartz-carbonate rocks. However, a threefold increase of potassium in the quartz-carbonate rocks, when compared to the FWS (Table III), indicates an influx of potassium into the quartz-carbonate rocks which led to the formation of fuchsite. According to data provided by Johannes (1969) it is estimated that the reaction described above took place at temperatures below 400°C.

The carbonate-rich transition zone between the FWS and the talc-carbonate rocks probably formed as a result of the reaction:



The silica released by this reaction was subsequently used for the formation of further talc-carbonate:



The introduction of CO_2 above was not sufficient to produce the chlorite-talc-carbonate rocks, because these required the exchange of further components from the underlying volcanics. A comparison with the chemistry of the FWS shows that the chlorite-talc-carbonate rocks are depleted in Mg and Ni, and enriched in Si, Ti, Al, Fe, and Ca. These findings agree with those of Sanford (1982) who showed that during mass transfer Si, Fe, and Ca are generally introduced into ultramafic bodies, while Mg and H_2O is lost from the ultramafics.

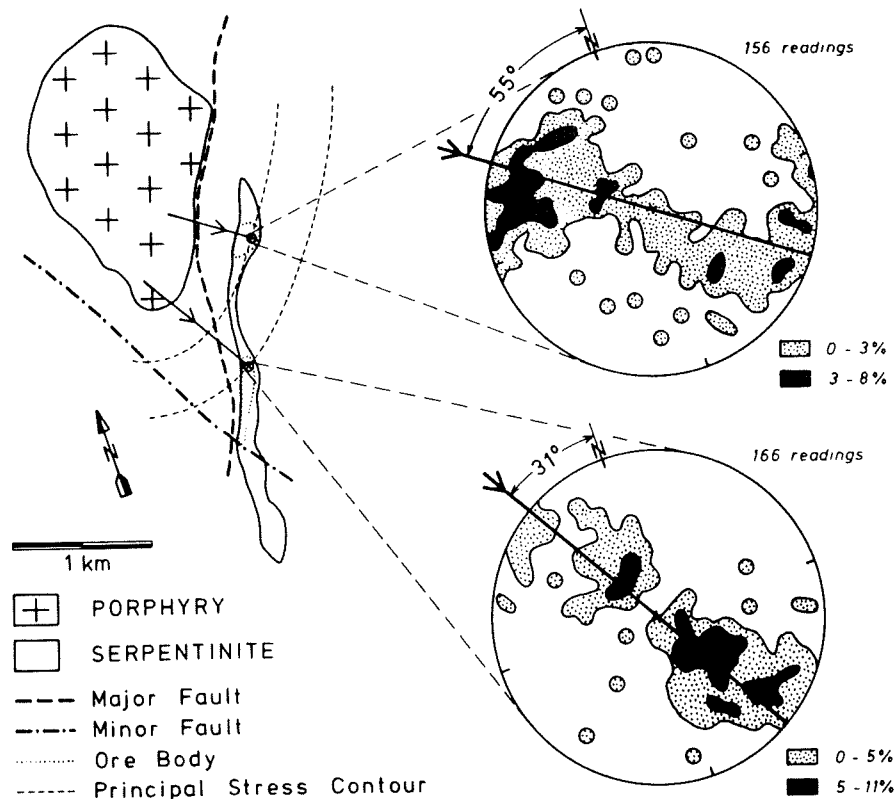


Figure 10 : Structural relationship between the fibre orientations of the chrysotile cross-fibre in the OZS and the position of the Northern Porphyry. Fibre orientations are plotted in equal area projection.

V. CONCLUSIONS

This study has shown that economic asbestos fibre grades in the Msauli ultramafic body are concentrated towards the central part of the serpentinite zone (OZS). Apart from high grades of chrysotile cross-fibre the OZS also contains appreciable amounts of brucite. Mineralogical differences encountered between the barren FWS and HWS and the fibre-bearing OZS are related to the optical properties of the serpentine species. In the FWS and HWS α -serpentine (lizardite) predominates in the olivine pseudomorphs, while the OZS consists chiefly of γ -serpentine (lizardite and chrysotile).

The Archaean Msauli ultramafic body appears to be comparable to most Phanerozoic ultramafic bodies. This is particularly so with regard to the mineralogical, geochemical and textural features noted, as well as the alteration effects recorded. Differences exist, however, with respect to the tectonic setting. Most ultramafic bodies in Phanerozoic belts are regarded as ophiolites, emplaced initially at mid-ocean ridges and closely related to plate tectonic processes (Coleman, 1977; Gass, 1982). Plate tectonic processes, such as those described for the Phanerozoic, probably did not occur during the Archaean (Kröner, 1981) but it is nevertheless suggested that the Msauli ultramafic body is closely analogous with Phanerozoic ophiolites.

ACKNOWLEDGMENTS

The author is indebted to Mr. O.H. Kuschke, Mr. H.H. Schaum, and Mr. J.C. Voigt of General Mining Union Corporation (GENCOR). Without their support this research would never have succeeded. Thanks are also due to Prof. C.R. Anhaeusser of the Economic Geology Research Unit and to Prof. R. Saager of the University of Cologne for their encouraging interest in this project. Finally, thanks are extended to Mrs. Doris Amaler for typing the manuscript.

REFERENCES

- Albee, A.L. (1962). Relationships between the mineral association, chemical composition and physical properties of the chlorite series. *Amer. Miner.*, 47, 851-870.
- Anhaeusser, C.R. (1976). The nature of chrysotile occurrences in southern Africa: a review: *Econ. Geol.*, 71, 96-116.
- (1978). The geological evolution of the primitive earth - evidence from the Barberton Mountain Land, 71-106. In: Tarling, D.H., Ed., *Evolution of the Earth's Crust*, Academic Press, London, 443 pp.
- (1979). Rodingite occurrences in some Archaean ultramafic complexes in the Barberton Mountain Land, South Africa. *Precambrian Res.*, 8, 49-76.
- (1981a). Geotectonic evolution of the Archaean successions in the Barberton Mountain Land, South Africa, 137-160. In: Kröner, A., Ed., *Precambrian Plate Tectonics*, Elsevier, Amsterdam, 781 pp.
- (1981b). The geology and evolution of the Barberton Mountain Land, 1-21. In: Anhaeusser, C.R., Ed., *Archaean Geology of the Barberton Mountain Land, Excursion Guidebook*. Geol. Soc. S. Afr., 78 pp.
- (1983). Archaean layered ultramafic complexes in the Barberton Mountain Land, South Africa. *Inform. Circ. Econ. Geol. Res. Unit, Univ. Witwatersrand, Johannesburg*, 161, 30 pp.
- Arndt, N.T., Naldrett, A.J., and Pyke, D.R. (1977). Komatiitic and iron-rich tholeiitic lavas of Munro township, northeast Ontario. *J. Petrol.*, 18, 319-369.
- Barton, J.M., Jr. (1983). Isotopic constraints on possible tectonic models for crustal evolution in the Barberton granite-greenstone terrane, southern Africa. *Spec. Publ. geol. Soc. S. Afr.*, 9, 73-79.
- Beswick, A.E. (1983). Primary fractionation and secondary alteration within an Archean ultramafic lava flow. *Contr. Miner. Petrol.*, 82, 221-231.
- Brindley, G.W., and Gillery, F.H. (1956). X-ray identification of chlorite species. *Amer. Miner.*, 41, 169-186.
- Brooks, C., and Hart, S.R. (1974). On the significance of komatiite. *Geology*, 2, 107-110.

- Büttner, W. (1983a). Mineralogische, geologische und geochemische Untersuchungen zur Genese der Msauli-Asbest-Lagerstätte, Barberton Greenstone Belt, Südafrika. Dissertation, Univ. Köln, 245 pp.
- (1983b). Untersuchungen zum Chemismus der Serpentinphasen in den Serpentiniten der Msauli-Asbest-lagerstätte. *Fortschr. Miner.*, 61, (1), 235-236.
- , and Saager, R., (1982a). The geology of the Msauli asbestos mine, Barberton Mountain Land, South Africa. *Erzmetall*, 35, 147-151.
- , and ----- (1982b). Rapid XRD determination of the chrysotile/lizardite ratios in asbestos-bearing serpentinites. *Ischermaks Miner. Petr. Mitt.*, 30, 177-187.
- , Barton, J.M. Jr., and Saager, R. (1983). Geochemistry, age and origin of some porphyry intrusions in the Onverwacht Group, Barberton greenstone belt. *Trans. geol. Soc. S. Afr.*, 86, 1-10.
- Chamberlain, J.A. (1966). Heazlewoodite and awaruite in serpentinites of the eastern townships, Quebec. *Can. Mineral.*, 8, 519-522.
- Chernosky, J.V. (1973). The stability of chrysotile $Mg_3Si_2O_{10}(OH)_4$. *Abstr. geol. Soc. Amer.*, 5, p.575.
- Chidester, A.H. (1962). Petrology and geochemistry of selected talc-bearing ultramafic rocks and adjacent country rocks in North-Central Vermont. *U.S. Geol. Surv. Prof. Pap.*, 345, 207 pp.
- Coleman, R.G. (1977). *Ophiolites - Ancient Oceanic Lithosphere?* New York, Springer Verlag, 229 pp.
- Cressey, B.A. (1979). Electron microscopy of serpentine textures, *Can. Mineral.*, 17, 741-756.
- De Waal, S.A., (1971). South African nickeliferous serpentinites. *Miner. Sci. Engng.*, 3, 32-45.
- Eckstrand, O.R. (1975). The Dumont serpentinite: a model for control of nickeliferous opaque mineral assemblages by alteration reactions in ultramafic rocks. *Econ. Geol.*, 70, 183-201.
- Eriksson, K.A. (1980). Transitional sedimentation styles in the Moodies and Fig Tree groups, Barberton Mountain Land, South Africa: evidence favouring an Archean continental margin. *Precambrian Res.*, 12, 141-160.
- Evans, B.W., Johannes, W., Oterdoom, H., and Trommsdorff, V. (1976). Stability of chrysotile and antigorite in the serpentinite multisystem. *Schweizerische Min. Petr. Mitt.*, 56, 79-93.
- Gass, I.G. (1982). Ophiolites. *Scient. Amer.*, 247, 108-117.
- Glen, R.A., and Butt, B.C. (1981). Chrysotile asbestos at Woodsreef. *Econ. Geol.*, 76, 1153-1169.
- Hajash, A. (1975). Hydrothermal processes along mid-ocean ridges: an experimental investigation. *Contr. Miner. Petrol.*, 53, 205-226.

- Hamilton, P.J., Evensen, N.M., O'Nions, R.K., Smith, H.S., and Erlank, A.J. (1979). Sm-Nd dating of Onverwacht group volcanics, southern Africa. *Nature*, 279, 298-300.
- Heinrichs, T. (1980). Lithostratigraphische Untersuchungen in der Fig Tree Gruppe des Barberton Greenstone Belt zwischen Umsoli und Lomati. *Göttinger Arbeiten Geol. Paläont.*, 22, 118 pp.
- Hess, H.H. (1933). The problem of serpentization and the origin of certain chrysotile asbestos, talc and soapstone deposits. *Econ. Geol.*, 28, 634-657.
- Hey, M.H. (1954). A new review of chlorites. *Miner. Mag.*, 30, 277-292.
- Hostetler, P.B., Coleman, R.G., and Mumpton, F. (1966). Brucite in alpine serpentinites. *Amer. Miner.*, 51, 75-98.
- Humphris, S.E., and Thompson, G. (1978). Hydrothermal alteration of oceanic basalts by seawater. *Geochim. cosmochim. Acta*, 42, 107-125.
- Ito, E., and Anderson, A.T. (1983). Submarine metamorphism of gabbros from the Mid-Cayman rise: petrographic and mineralogic constraints on hydrothermal processes at slow-spreading ridges. *Contr. Miner. Petrol.*, 82, 371-388.
- Jahn, B., Gruau, G., and Glikson, A.Y. (1982). Komatiites of the Onverwacht Group, S. Africa: REE geochemistry, Sm/Nd age and mantle evolution. *Contr. Miner. Petrol.*, 80, 25-40.
- Johannes, W. (1968). Experimental investigation of the reaction forsterite + H_2O = serpentine + brucite. *Contr. Miner. Petrol.*, 19, 309-315.
- (1969). An experimental investigation of the system MgO - SiO_2 - H_2O - CO_2 . *Amer. J. Sci.*, 267, 1083-1104.
- Kröner, A. (Ed.) (1981). *Precambrian Plate Tectonics*. Amsterdam, Elsevier, 402 pp.
- Laubscher, D.H. (1964). The occurrence and origin of chrysotile asbestos and associated rocks, Shabani, Southern Rhodesia, 593-624. In: Haughton, S.H., Ed., *Geology of Some Ore Deposits in Southern Africa*. *Geol. Soc. S. Afr.*, 2, 739 pp.
- LeMaitre, R.W. (1976). The chemical variability of some common igneous rocks. *J. Petrol.*, 17, 589-637.
- Liou, J.G., and Ernst, W.G. (1979). Oceanic ridge metamorphism of the east Taiwan ophiolite. *Contr. Miner. Petrol.*, 68, 335-348.
- Lofgren, G.E. (1983). Effect of heterogeneous nucleation on basaltic textures: a dynamic crystallization study. *J. Petrol.*, 24, 229-255.
- , and Donaldson, C.D. (1975). Curved branching crystals and differentiation in comb-layered rocks. *Contr. Miner. Petrol.*, 49, 309-319.
- Lowe, D.R., and Knauth, L.P. (1977). Sedimentology of the Onverwacht Group (3.4 billion years), Transvaal, South Africa, and its bearing on the characteristics and evolution of the early earth. *J. Geol.*, 85, 699-723.

- Moh, G.H., and Kullerud, G. (1982). The Cu-Ni-S system and low temperature mineral assemblages, 677-688. In: Amstutz, G.C., et al., Eds., *Ore Genesis - State of the Art*, Berlin, Springer Verlag.
- Moody, J.B. (1976). An experimental study on the serpentinization of iron-bearing olivines. *Can. Mineral.*, 14, 462-478.
- Prichard, H.M. (1979). A petrographic study of the process of serpentinization in ophiolites and the ocean crust. *Contr. Miner. Petrol.*, 68, 231-241.
- Pyke, D.R., Naldrett, A.J., and Eckstrand, O.R. (1973). Archean ultramafic flows in Munro township, Ontario. *Bull. geol. Soc. Amer.*, 84, 955-978.
- Ramdohr, P. (1975). *Die Erzmineralien und ihre Verwachsungen*. Berlin, Akademie Verlag, 1277 pp.
- Ramsay, J.G. (1980). The crack-seal mechanism of rock deformation. *Nature*, 284, 135-139.
- Sanford, R.F. (1982). Growth of ultramafic reaction zones in greenschist to amphibolite facies metamorphism: *Amer. J. Sci.*, 282, 543-616.
- Seyfried, W.E., and Dibble, W.E. (1980). Seawater-peridotite interaction at 300°C and 500 bars: implications for the origin of oceanic serpentinites. *Geochim. cosmochim. Acta*, 44, 309-321.
- Tertsch, H. (1922). Student am Westrande des Dunkelsteiner Granulitmassives. *Tschermaks Miner. Petro. Mitt.*, 35, 177-214.
- Tröger, W.E. (1969). *Optische Bestimmung der Gesteinsbildenden Minerale*. Teil 2, Stuttgart, Schweizerbart'sche Verlagshandlung, 822 pp.
- Turner, F.J., and Verhoogen, J. (1960). *Igneous and Metamorphic Petrology*. New York, McGraw-Hill, 694 pp.
- Van Biljon, W.J. (1964). The chrysotile deposits of the eastern Transvaal and Swaziland, 625-669. In: Haughton, S.H., Ed., *Geology of Some Ore Deposits in Southern Africa*. *Geol. Soc. S. Afr.*, 2, 739 pp.
- Viljoen, M.J., and Viljoen, R.P. (1969a). An introduction to the geology of the Barberton granite-greenstone terrain. *Spec. Publ. geol. Soc. S. Afr.*, 2, 9-28.
- , and ----- (1969b). The geology and geochemistry of the lower ultramafic unit of the Onverwacht group and a proposed new class of igneous rocks. *Spec. Publ. geol. Soc. S. Afr.*, 2, 55-85.
- Viljoen, R.P., and Viljoen, M.J. (1969c). The geological and geochemical significance of the upper formations of the Onverwacht group. *Spec. Publ. geol. Soc. S. Afr.*, 2, 113-152.
- , and ----- (1970). The geology and geochemistry of the layered ultramafic bodies of the Kaapmuiden area, Barberton Mountain Land. *Spec. Publ. geol. Soc. S. Afr.*, 1, 661-688.

- Wenner, D.B. (1979). Hydrogen, oxygen and carbon isotopic evidence for the origin of rodingites in serpentinitized ultramafic rocks. *Geochim. cosmochim. Acta*, 43, 603-614.
- , and Taylor, H.P. (1971). Temperatures of serpentinitization of ultramafic rocks based on D/H / O^{18}/O^{16} fractionation between coexisting serpentine. *Contr. Miner. Petrol.*, 32, 165-185.
- , and ----- (1973). Oxygen and hydrogen isotope studies of the serpentinitization of ultramafic rocks in oceanic environments and continental ophiolite complexes. *Amer. J. Sci.*, 273, 207-239.
- , and ----- (1974). D/H and O^{18}/O^{16} studies of serpentinitization of ultramafic rocks. *Geochim. cosmochim. Acta*, 38, 1255-1286.
- Wetzel, R. (1973). Chemismus and physikalische Parameter einiger Chlorite aus der Grünschieferfazies. *Schweizerische Min. Petr. Mitt.*, 53, 273-298.
- Whittaker, E.J.W., and Zussman, J. (1956). The characterization of serpentine minerals by X-ray diffraction. *Miner. Mag.*, 31, 107-126.
- Wicks, F.J. (1979). Mineralogy, chemistry and crystallography of chrysotile asbestos. *Short Course Handbk. Miner. Assoc. Can.*, 4, 35-78.
- , and Whittaker, E.J.W. (1977). Serpentine textures and serpentinitization. *Can. Mineral.*, 15, 459-488.
- , and Zussman, J. (1977). An idealized model for serpentine textures after olivine. *Can. Mineral.*, 15, 446-458.
- Williams, D.A.C., and Hallberg, J.A. (1973). Archaean layered intrusions of Eastern Goldfields region, Western Australia. *Contr. Miner. Petrol.*, 38, 45-70.
- Yada, K., and Iishi, K. (1974). Serpentine minerals hydrothermally synthesized and their microstructures. *J. Crystal Growth*, 24/25, 627-630.
- , and ----- (1977). Growth and microstructure of synthetic chrysotile. *Amer. Mineral.*, 62, 958-965.